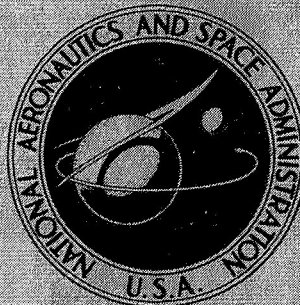


N68-35764

NASA TECHNICAL  
MEMORANDUM



NASA TM X-1653

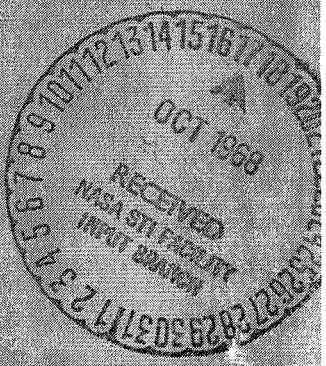
NASA TM X-1653

STATIC PERFORMANCE OF AN  
AUXILIARY INLET EJECTOR NOZZLE  
FOR SUPERSONIC-CRUISE AIRCRAFT

by George D. Shrewsbury and John R. Jones

Lewis Research Center  
Cleveland, Ohio

NATIONAL AERONAUTICS AND SPACE ADMINISTRATION • WASHINGTON, D. C. • OCTOBER 1968



STATIC PERFORMANCE OF AN AUXILIARY INLET EJECTOR  
NOZZLE FOR SUPERSONIC-CRUISE AIRCRAFT

By George D. Shrewsbury and John R. Jones

Lewis Research Center  
Cleveland, Ohio

NATIONAL AERONAUTICS AND SPACE ADMINISTRATION

---

For sale by the Clearinghouse for Federal Scientific and Technical Information  
Springfield, Virginia 22151 - CFSTI price \$3.00

## ABSTRACT

A model of an auxiliary inlet ejector nozzle was tested in the Lewis Research Center's static test facility over a range of nozzle pressure ratios of approximately 1.5 to 17. The model diameter was 33 cm. Secondary flows of from 0 to 10 percent of the primary nozzle flow were investigated. Configurations simulating takeoff, transonic acceleration, supersonic acceleration, and supersonic cruise were tested. The takeoff configurations were evaluated with and without noise suppressor chutes.

STATIC PERFORMANCE OF AN AUXILIARY INLET EJECTOR  
NOZZLE FOR SUPERSONIC-CRUISE AIRCRAFT  
by George D. Shrewsbury and John R. Jones  
Lewis Research Center

SUMMARY

A model of an auxiliary inlet ejector nozzle was tested in the Lewis Research Center's static test facility over a range of nozzle pressure ratios of approximately 1.5 to 17. The model diameter was 33 centimeters. Secondary flows of from 0 to 10 percent of the primary nozzle flow were investigated. Configurations simulating takeoff, transonic acceleration, supersonic acceleration, and supersonic cruise were tested. The takeoff configurations were evaluated with and without noise suppressor devices.

By extrapolating the results to a nozzle pressure ratio of 29.0 (corresponding to supersonic cruise), the nozzle efficiency was estimated to be 0.9855 at a corrected secondary flow ratio of 0.02. This performance was obtained with a large internal shroud diameter and large shroud cooling slot area. At a corrected secondary flow ratio of 0.02, reducing the internal shroud diameter reduced the extrapolated nozzle efficiency for both the supersonic-cruise and supersonic-acceleration geometries. Increasing the size of the shroud cooling slot increased the extrapolated nozzle efficiencies and decreased the total pressure required to pump a given secondary flow at the supersonic-cruise condition.

The installation of noise suppressor chutes reduced the nozzle efficiencies for the takeoff configurations between 13 and 26 percent, depending on the chute configuration and chute angle. A secondary total pressure of 98 percent free-stream total pressure is required to provide a secondary flow ratio of 0.02 with the takeoff configurations. For secondary flow ratios of 0.04 and greater, secondary total pressures greater than free-stream are required. The chutes had little effect on pumping characteristics.

INTRODUCTION

As part of a broad program in airbreathing propulsion, the Lewis Research Center is

evaluating various exhaust nozzle concepts appropriate for supersonic cruise aircraft. These nozzles must operate efficiently over a wide range of flight conditions and engine power settings. Requirements such as these usually necessitate extensive variations in nozzle geometry, including both the primary and secondary nozzle areas. The performance of a variable flap ejector and a low-angle plug nozzle designed for a supersonic-cruise aircraft are reported in references 1 and 2. Another nozzle type of interest is the auxiliary inlet ejector. At the supersonic cruise point, this nozzle operates like the variable flap ejector. At takeoff and subsonic flight conditions, auxiliary inlets open to admit tertiary air to prevent the nozzle from overexpanding. Since this tertiary air fills part of the shroud, there is a reduced requirement for exit area variation and a corresponding reduction in boattail angle.

This report documents the internal performance of an auxiliary inlet ejector nozzle suitable for an afterburning turbojet engine designed for cruise at a Mach number near 2.7. A model with a 33-centimeter diameter was tested in the Lewis Research Center's static test facility over a range of nozzle pressure ratios from approximately 1.5 to 17. Secondary flow was varied from 0 to 10 percent of primary nozzle flow. Configurations simulating takeoff, transonic acceleration, supersonic acceleration, and supersonic cruise were tested. The takeoff configurations were evaluated with and without noise suppression devices. Dry air at room temperature was used for primary, secondary, and tertiary flows.

## SYMBOLS

A	area
$C_D$	discharge coefficient
d	diameter
F	thrust
$F'$	stream thrust parameter, $(m_p V_{p,9} + m_s V_{s,9} + p_9 A_9)/P_7 A_8$
$F_{ip}$	ideal primary thrust based on measured primary flow
$F_{is}$	ideal secondary thrust based on measured secondary flow
$F/(F_{is} + F_{ip})$	nozzle efficiency
h	height
$l$	length
m	mass flow rate

P	total pressure
p	static pressure
V	velocity
x	axial distance
$\theta$	noise suppressor chute angle
$\tau$	ratio of secondary to primary total temperatures
$\varphi$	primary nozzle flap angle
$\omega$	ratio of secondary to primary flow rate
$\omega\sqrt{\tau}$	corrected secondary flow ratio

Subscripts:

c	chute
i	ideal
p	primary
s	secondary
0	free stream
7	primary nozzle inlet station
8	primary nozzle throat station
9	ejector shroud exit station
*	sonic conditions

## APPARATUS

Table I lists the geometric variables of each nozzle configuration. The configurations are grouped in the table to correspond to various simulated flight regimes. Each configuration is identified by a two-digit number: the first digit indicates the primary nozzle and the second indicates the shroud. Primary nozzle geometry is identified in figure 1 where its diameter, flap length, and angle are shown corresponding to three power settings. These primary nozzles simulate a continuously variable nozzle which is positioned by actuators for various engine power settings. Figure 2 is a photograph of a typical primary nozzle assembly showing the simulated actuators. Details of the shrouds are shown in figure 3. Four different exit areas were used which corresponded to discrete positions of a continuously variable multiple flap shroud downstream of the cooling air slot. Upstream of the slot the shroud geometry was assumed fixed although two shapes (corre-

sponding to variations in  $d_s$ ) were tested. Six shroud configurations were required since the cooling slot height was changed on the shrouds with maximum exit area. Details of the auxiliary inlet section are shown in figure 4. Sixteen single-hinge doors were tested either in the full-open or closed positions. When open, the inlet area measured normal to the door surface was 226.8 square centimeters.

The takeoff nozzle configurations were also evaluated with six noise suppressor chutes installed. A photograph of an aft view of such an assembly is shown in figure 5. Sketches and photographs of the various chute geometries are presented in figures 6(a) and (b), respectively. Details of the noise suppressor configurations are tabulated in table II. Although effects of these chutes on nozzle thrust and pumping characteristics were determined in the present study, noise suppression capabilities were not determined.

A schematic diagram of the static test facility showing the nozzle support and air supply systems is presented in figure 7. A load cell was used to measure the net force on the free parts of the system; tare forces were then removed to obtain the gross thrust. A rake located at station 7 was used to calculate an area-weighted average of primary nozzle inlet total pressure. Data reduction methods described in reference 1 were used. The sketch also shows the location of the  $p_0$  measurement. Figure 8 presents a photograph of a test nozzle installed in the facility. This particular configuration shows the auxiliary inlets in the open position.

Figure 9 is a sketch showing instrumentation details on the auxiliary inlet ejector nozzle. A tabulated listing is given showing the location of static pressure taps on the internal portion of the shroud. The approximate position of the secondary total pressure rake is also shown.

## PROCEDURE

A 21.34-centimeter diameter ASME calibration nozzle with an ideal flow coefficient of 0.9938 was tested in the static test facility in preparation for the auxiliary inlet ejector test program. Figure 10 shows a comparison of measured performance characteristics in the static test facility of the calibration nozzle with its calculated performance curves based on the ideal flow coefficient. The comparison shows nozzle efficiency, flow coefficient, and stream thrust parameter as a function of primary nozzle pressure ratio. In general, the agreement is good.

A total of 21 auxiliary inlet ejector nozzle configurations were tested simulating the following flight conditions:

- (1) Takeoff with maximum reheat, with and without noise suppressors (configurations 12, 13, 14, and 15 with doors open)

(2) Takeoff at a reduced engine power setting without noise suppressors (configuration 34)

(3) Transonic acceleration (configurations 12, 13, and 14 with doors closed)

(4) Supersonic acceleration (configurations 11 and 15 with doors closed)

(5) Supersonic cruise (configurations 21, 25, and 26)

The testing procedure for each configuration was similar. Each was tested over a range of nozzle pressure ratios varying from 1.5 to about 17 at corrected secondary weight flow ratios of 0, 0.02, 0.04, and 0.10.

Values of nozzle efficiency and ejector pumping characteristics are presented for each configuration tested. For the supersonic acceleration and supersonic cruise configurations, measured stream thrust parameters, primary nozzle flow coefficients, and pumping characteristics were used to extrapolate for values of nozzle efficiency at pressure ratios greater than those recorded. The expression  $F/(F_{ip} + F_{is})$  was used for nozzle efficiency in this report. In cases where  $P_s/p_0$  was less than 1.0,  $F_{is}$  was set equal to zero. Data where  $F_{is}$  was set equal to zero are indicated in the figures. If nozzle efficiency in the form  $F/F_{ip}$  is preferred, it may be obtained by using:

$$\frac{F}{F_{ip}} = \frac{F}{F_{ip} + F_{is}} \left[ 1 + \frac{C_{F_{is}}}{C_{F_{ip}}} \omega \sqrt{\tau} \right]$$

where

$$C_{F_{is}} = \frac{F_{is}}{P_s A_s^*}$$

and

$$C_{F_{ip}} = \frac{F_{ip}}{P_p A_p^*}$$

Values of  $C_{F_{is}}$  and  $C_{F_{ip}}$  are usually tabulated in compressible flow tables as functions of the pressure ratio of each stream, and the pumping characteristics are presented in the data of the report.

## RESULTS AND DISCUSSION

### Supersonic-Cruise Configurations

Figure 11 shows the performance characteristics for the supersonic-cruise configurations of the auxiliary inlet ejector nozzle. Nozzle efficiencies and secondary flow pumping characteristics are presented up to a nozzle pressure ratio of approximately 17. Configuration 21, which had a small internal shroud diameter, showed a hysteresis effect at zero secondary flow. Stream thrust parameters and primary nozzle flow coefficients for the supersonic-cruise configurations are presented in figure 12. Figure 13 shows the extrapolated performance of the supersonic-cruise configurations. Values of  $P_s/P_7$ ,  $F'$ , and  $C_{D8}$  for design pressure ratios were extrapolated from the data of figures 11 and 12. Extrapolated values of nozzle efficiency were calculated from:

$$\frac{F}{F_{ip} + F_{is}} = \frac{F'(P_7 A_8) - A_9 p_0}{F_{ip} + F_{is}}$$

where  $F_{ip}$  and  $F_{is}$  are based on measured flow rate and the pressure ratio being considered. The extrapolation simply corrects the  $p_0 A_9$  term for higher pressure ratios. Of the supersonic-cruise configurations tested, the maximum nozzle efficiency at a nominal corrected secondary flow ratio of 0.02 was obtained with configuration 26 and had a value of 0.9855 at a nozzle pressure ratio of approximately 29.0. Figure 14 shows the effect of internal shroud diameter on the extrapolated performance of the auxiliary inlet ejector nozzle at supersonic cruise with a corrected secondary flow ratio of 0.02. Data are shown for configurations 21 and 25. For the data shown, the reduced internal shroud diameter reduces the peak extrapolated nozzle efficiency by about 0.30 percent. Figure 15 shows the effect of internal shroud diameter on the internal pressure distribution. Reducing the shroud diameter creates higher pressures on the forward facing portion of the shroud causing a drag.

The effect of cooling slot size on extrapolated performance is shown in figure 16. Data are shown for a corrected secondary flow ratio of 0.02 for the supersonic-cruise configurations with the large internal shroud diameter. Increasing the size of the cooling slot increases the peak extrapolated nozzle efficiency for the data shown. Figure 17 shows the effect of cooling slot size on the pumping characteristics of the auxiliary inlet ejector nozzle. Data are shown for the supersonic-cruise configurations with the large internal shroud diameter extrapolated to design pressure ratios. Increasing the cooling slot size reduces the total pressure required to pump a given secondary flow over the entire range of secondary flow ratios investigated.

## Supersonic Acceleration Configurations

Performance characteristics of the supersonic-acceleration configurations are presented in figure 18. Nozzle efficiencies and pumping characteristics are shown for configurations 11 and 15 up to nozzle pressure ratios of approximately 13. Configuration 11 which had a small internal shroud diameter, demonstrated marked hysteresis effects near the breakaway pressure ratio of the nozzle. The hysteresis effects were small, however, at the higher nozzle pressure ratios. Figure 19 shows the stream thrust parameter and primary nozzle flow coefficient for the supersonic-acceleration configurations. The performance of the supersonic-acceleration configurations when extrapolated to higher pressure ratios is presented in figure 20. Nozzle efficiencies were extrapolated using extrapolated values of  $P_s/P_7$ ,  $F'$ , and  $C_{D8}$  from figures 18 and 19.

The effect of internal shroud diameter on the extrapolated performance of the supersonic-acceleration configurations is shown in figure 21. Data are shown for a corrected secondary flow ratio of 0.02. The reduced internal shroud diameter reduces the peak nozzle efficiency by approximately 0.10 percent.

## Transonic Acceleration Configurations

The performance characteristics of the transonic acceleration configurations of the auxiliary inlet ejector nozzle are shown in figure 22. Data are shown for configurations 14, 13, and 12, with doors closed, at various corrected secondary flow ratios. The performance values given are for internal performance only and do not include external flow effects on boattail drag.

## Takeoff Configurations

The performance characteristics of the takeoff configurations without noise suppression are presented in figure 23. Configurations utilizing maximum reheat and also no reheat are presented. Closing the inlets, in either case, greatly improves the pumping characteristics of the nozzle but reduces the nozzle efficiency considerably at a nominal takeoff pressure ratio of 3.0. Some hysteresis effects were observed on configuration 34, with doors both open and closed. On the configurations with auxiliary inlets open, the nozzle efficiency exceeds an ideal value of 1.00. This occurs because the tertiary flow being admitted through the auxiliary inlets is not accounted for in the ideal thrust.

The performance characteristics of the takeoff configurations with noise suppressor chutes are presented in figure 24. The presence of the noise suppressor chutes drastically

ly reduces the nozzle efficiency for all configurations investigated when compared to configuration 14 without chutes. Increasing the angle of the flat noise suppressor chute further reduces the nozzle efficiency at a pressure ratio of 3.0. At a flat chute angle of  $25^{\circ}$ , the noise suppressor reduces the nozzle efficiency approximately 18 percent at a nozzle pressure of 3.0. At a flat chute angle of  $40^{\circ}$ , the noise suppressor chute reduces the nozzle efficiency approximately 26 percent at a nozzle pressure ratio of 3.0.

Of the three noise suppressor types investigated, the V2 configuration gave a slightly higher performance, reducing the nozzle efficiency only 13 percent at a pressure ratio of 3.0. The V1 and V2 configurations were both superior to the flat chute design in nozzle performance. The presence of the noise suppressors had little or no effect on the secondary pumping characteristics of the takeoff configurations with maximum reheat primary nozzles.

Figure 25 shows the effect of noise suppressor chutes on secondary shroud pressure distributions at a nozzle pressure ratio of 3.0. Data are shown for a corrected secondary flow ratio of 0.04. If the ejector shroud is free to move, it will assume a geometry near that of configuration 14 without noise suppressors if a pressure near  $p_0$  exists on the external portion of the boattail. With noise suppressors, the ejector will assume a geometry near that of configuration 13. It is concluded that the presence of the noise suppressor chute would cause a free-floating ejector to assume a larger area ratio at the takeoff pressure ratio.

Figure 26 shows the secondary total pressure recovery requirements for different flight regimes. The nozzle pressure ratios, free-stream Mach numbers, and configurations indicated on the figure were selected as representative of the various flight regimes. The secondary air total pressure recovery was calculated using the free-stream Mach number, nozzle pressure ratio, and typical auxiliary inlet ejector pumping characteristics for each flight condition. The secondary pumping characteristics were relatively constant for each flight condition. It is obvious from the data that the pumping characteristics for the takeoff configuration are marginal. A pressure recovery of 98 percent free-stream total pressure is required to provide a secondary flow ratio of 0.02. For secondary weight flow ratios of 0.04 and greater, an air supply with a total pressure greater than free stream, such as engine compressor bleed, will be required.

## SUMMARY OF RESULTS

A model of an auxiliary inlet ejector nozzle was tested in the Lewis Research Center's static test facility over a range of nozzle pressure ratios of approximately 1.5 to 17. The model diameter was 33 centimeters. Secondary flows of from 0 to 10 percent of the primary nozzle flow were investigated. Models simulating takeoff, transonic ac-

celeration, supersonic acceleration, and supersonic cruise configurations were tested. The takeoff configurations were evaluated with and without noise suppressor devices. Dry air at room temperature was used for primary, secondary, and tertiary flows. The following observations were made:

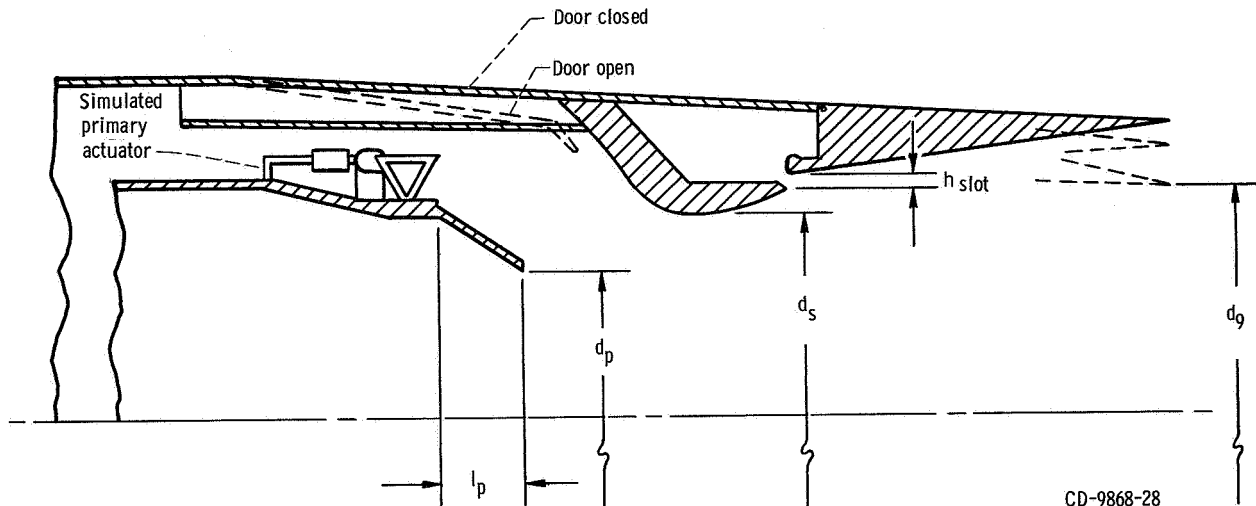
1. By extrapolating the results to a nozzle pressure ratio of 29.0 (corresponding to supersonic cruise), the nozzle efficiency was estimated to be 0.9855 at a corrected secondary flow ratio of 0.02. This performance was obtained with a large internal shroud diameter and large ejector shroud cooling slot area (configuration 26).
2. At a corrected secondary flow ratio of 0.02, reducing the ratio of internal shroud to primary nozzle diameter from 1.421 to 1.370 reduced the extrapolated nozzle efficiency 0.30 percent for the supersonic-cruise geometry. At the supersonic-acceleration condition, reducing the shroud diameter ratio from 1.245 to 1.200 reduced the nozzle efficiency 0.10 percent. At the same corrected secondary flow, the reduced shroud diameter increased the total pressure required to pump a given secondary flow for both the supersonic-cruise and supersonic-acceleration configurations. Hysteresis effects on nozzle efficiency were observed on the supersonic-acceleration and supersonic-cruise configurations when the reduced shroud diameter was used.
3. Increasing the size of the ejector shroud cooling slot from 0 to 15.916 square centimeters increased the extrapolated nozzle efficiencies for the supersonic cruise configurations at a corrected secondary flow of 0.02. Increasing the slot size also reduced the total pressure required to pump a given secondary flow at design pressure ratios.
4. Installing noise suppressor chutes severely reduced nozzle efficiencies on the takeoff configurations. The maximum reduction at a nozzle pressure ratio of 3.0 was 26 percent for a flat chute at an angle of  $40^{\circ}$ . Reducing the chute angle decreased the reduction in nozzle efficiency. The flat chute at an angle of  $25^{\circ}$  reduced the efficiency 18 percent. The V1 and V2 chute configurations reduced the nozzle efficiency approximately 13 percent. Little or no effect was observed on takeoff pumping characteristics.
5. Pumping characteristics for the takeoff configurations are marginal. A secondary total pressure of 98 percent free-stream total is required to provide a secondary flow ratio of 0.02. For secondary weight flow ratios of 0.04 and greater, an air supply with a total pressure greater than free-stream total, such as engine compressor bleed, will be required.

Lewis Research Center,  
National Aeronautics and Space Administration,  
Cleveland, Ohio, May 17, 1968,  
126-15-02-10-22.

## REFERENCES

1. Steffen, Fred W.; and Jones, John R.: Performance of a Wind Tunnel Model of an Aerodynamically Positioned Variable Flap Ejector at Mach Numbers from 0 To 2.0. NASA TM X-1639, 1968.
2. Bresnahan, Donald L.; and Johns, Albert L.: Cold Flow Investigation of a Low Angle Turbojet Plug Nozzle With Fixed Throat and Translating Shroud at Mach Numbers From 0 To 2.0. NASA TM X-1619, 1968.

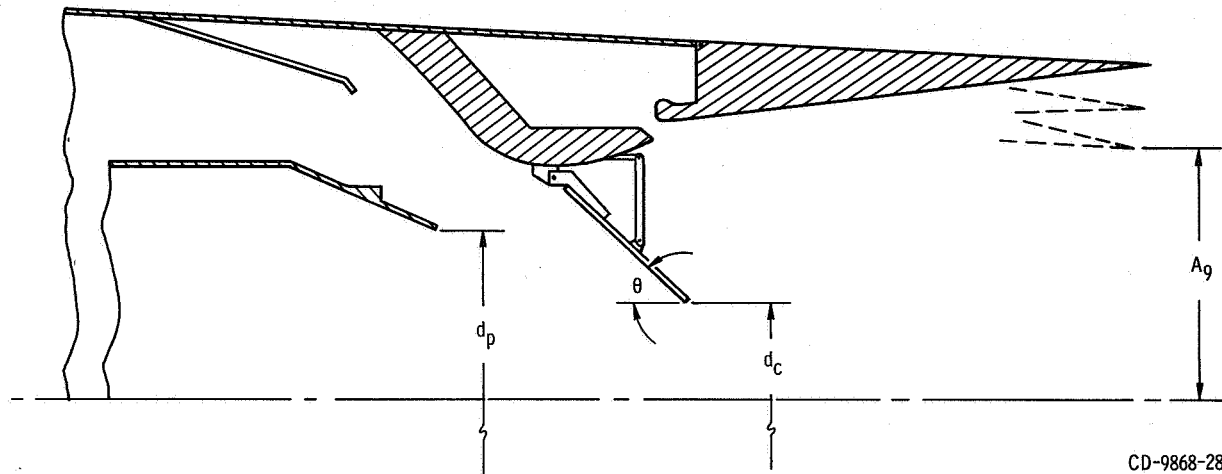
TABLE I. - AUXILIARY INLET EJECTOR NOZZLE CONFIGURATIONS

[Auxiliary inlet area,  $226.8 \text{ cm}^2$  (measured normal to door surface).]

Con- figura- tion	Primary nozzle diameter, $d_p$ , cm	Ejector shroud exit station diameter, $d_9$ , cm	Primary nozzle area, $A_p$ , $\text{cm}^2$	Area at ejector shroud exit station, $A_9$ , $\text{cm}^2$	Minimum shroud diameter, $d_s$ , cm	Slot height, $h_{\text{slot}}$ , cm	Slot area, $A_{\text{slot}}$ , $\text{cm}^2$	Primary nozzle length, $l_p$ , cm	Inlet posi- tion	Flight regime
21	17.66	33.03	244.88	856.72	24.21	0.132	11.01	5.273	Closed	Supersonic cruise
26	17.66	33.03	244.88	856.72	25.10	.185	15.92	5.273	Closed	
25	17.66	33.03	244.88	856.72	25.10	.112	9.568	5.273	Closed	
25	17.66	33.03	244.88	856.72	25.10	0	0	5.273	Closed	
11	20.18	33.03	319.76	856.72	24.21	0.132	11.01	5.750	Closed	Supersonic acceleration
15	20.18	33.03	319.76	856.72	25.10	.112	9.568	5.750	Closed	
14	20.18	25.45	319.76	508.73	25.10	0.112	10.43	5.750	Closed	Transonic acceleration
13	20.18	27.90	319.76	611.32	25.10	.114	9.787	5.750	Closed	
12	20.18	31.08	319.76	758.75	25.10	.114	9.787	5.750		
34	17.26	25.45	233.95	508.73	25.10	0.122	10.43	5.156	Open	Takeoff
34	17.26	25.45	233.95	508.73	25.10	.122	10.43	5.156	Closed	
14	20.18	25.45	319.76	508.73	25.10	.122	10.43	5.750	Open	
13	20.18	27.90	319.76	611.32	25.10	.114	9.787	5.750	Open	
12	20.18	31.08	319.76	758.75	25.10	.114	9.787	5.750	Open	
13	20.18	27.90	319.76	611.32	25.10	0.124	10.65	5.750	Open	Takeoff with noise sup- pressors
<sup>a</sup> 12	20.18	31.08	319.76	758.75	25.10	.127	10.86	5.750	Open	
15	20.18	33.03	319.76	856.72	25.10	.127	10.87	5.750	Open	

<sup>a</sup>Tested with 5 different noise suppressor chute geometries.

TABLE II. - DETAILS OF NOISE SUPPRESSOR  
CONFIGURATIONS TESTED



Configuration	Area at ejector shroud exit station, $A_9$ , $\text{cm}^2$	Chute geometry	Chute description		
			Noise suppressor chute angle, $\theta$	Penetra- tion, <sup>a</sup> percent	Blockage, <sup>b</sup> percent
13	611.32	Flat	$32^{\circ}40'$	50	25.3
12	758.75	Flat	$32^{\circ}40'$	50	25.3
15	856.72	Flat	$32^{\circ}40'$	50	25.3
12	758.75	Flat	$25^{\circ}$	35	20.2
12	758.75	Flat	$40^{\circ}$	64	29.7
12	758.75	V1	$32^{\circ}40'$	50	25.3
12	758.75	V2	$32^{\circ}40'$	50	25.3

<sup>a</sup>Percentage of penetration,  $\left(1 - \frac{d_c}{d_p}\right) 100$ .

<sup>b</sup>Percentage of blockage,  $\left(\frac{\text{Chute projected area}}{A_p}\right) 100$ .

Primary nozzle	Primary nozzle length, $l_p$	Primary nozzle diameter, $d_p$	Power setting	Primary nozzle flap angle, $\varphi$ , deg
1	5.750	20.178	Maximum reheat	13°45°
2	5.273	17.658	Nominal reheat	26°50°
3	5.156	17.259	Dry, reduced power setting	29°05°

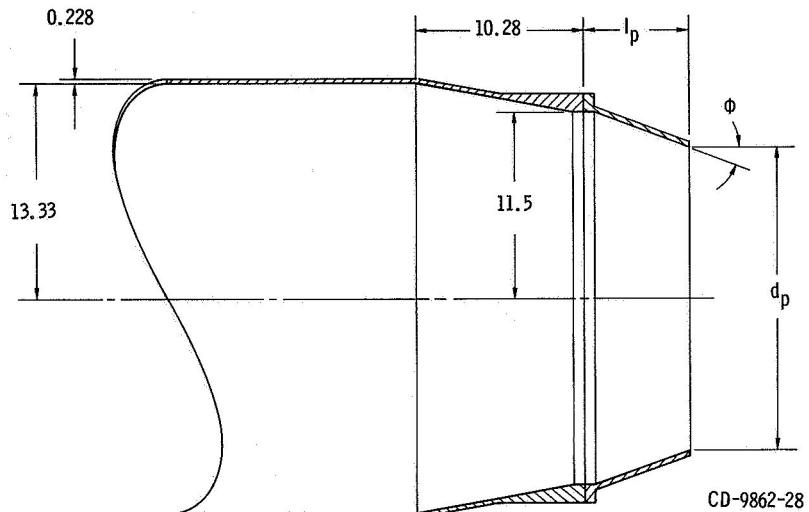
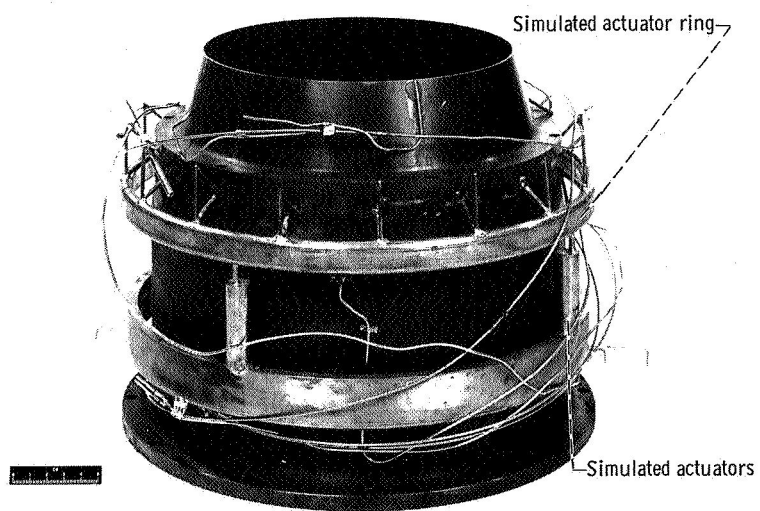
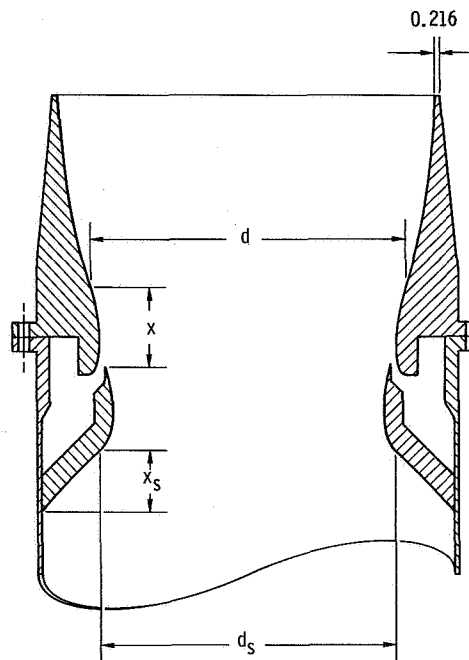


Figure 1. - Auxiliary inlet ejector primary nozzle details. (All dimensions in centimeters.)



C-67-4018

Figure 2. - Primary nozzle assembly showing simulated actuators.



CD-9863-28

Secondary nozzle axial distance, $x_s$	Minimum shroud diameter	
	$a_{d_s, 1}$	$d_{s, 2}$
0	37.10	37.10
1.80	35.00	35.00
3.59	31.92	31.92
4.48	29.63	29.63
6.29	26.05	26.64
8.08	24.38	25.29
8.98	24.22	25.10
11.14	24.74	25.54
14.73	26.31	27.00

<sup>a</sup>Contour used only with shroud 1.

Axial distance, $x$	Diameter, $d$	Axial distance, $x$	Diameter, $d$
Shroud 1		Shroud 4	
0	26.65	0	27.35
2.62	27.70	2.62	27.35
6.93	29.20	6.93	27.38
11.23	30.50	11.23	27.41
15.55	31.65	15.55	27.25
19.85	32.60	19.85	26.65
23.41	33.03	23.60	25.45
Shroud 2		Shroud 5	
0	27.35	0	27.35
2.62	28.05	2.62	28.25
6.93	29.00	6.93	29.60
11.23	29.82	11.23	30.75
15.55	30.52	15.55	31.75
19.85	31.05	19.85	32.63
23.52	31.08	23.41	33.03
Shroud 3		Shroud 6	
0	27.35	0	27.51
2.62	27.68	2.62	28.47
6.93	28.05	6.93	29.78
11.23	28.30	11.23	30.92
15.55	28.45	15.55	31.95
19.85	28.41	19.85	32.78
23.60	27.90	23.41	33.03

Figure 3. - Ejector nozzle. (All dimensions in centimeters.)

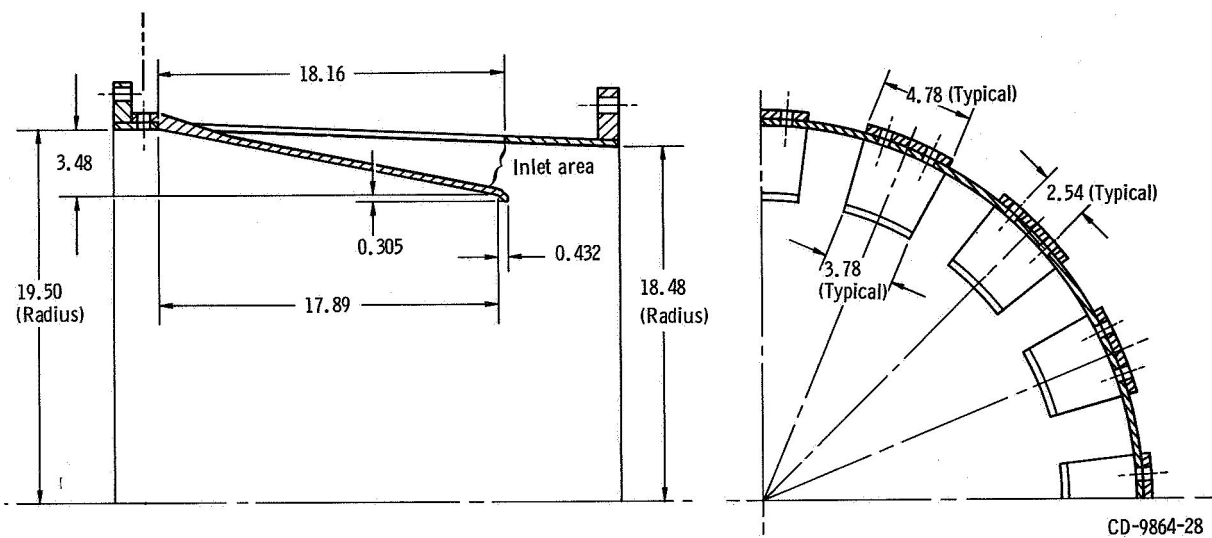


Figure 4. - Details of auxiliary inlet section. (All dimensions in centimeters.)

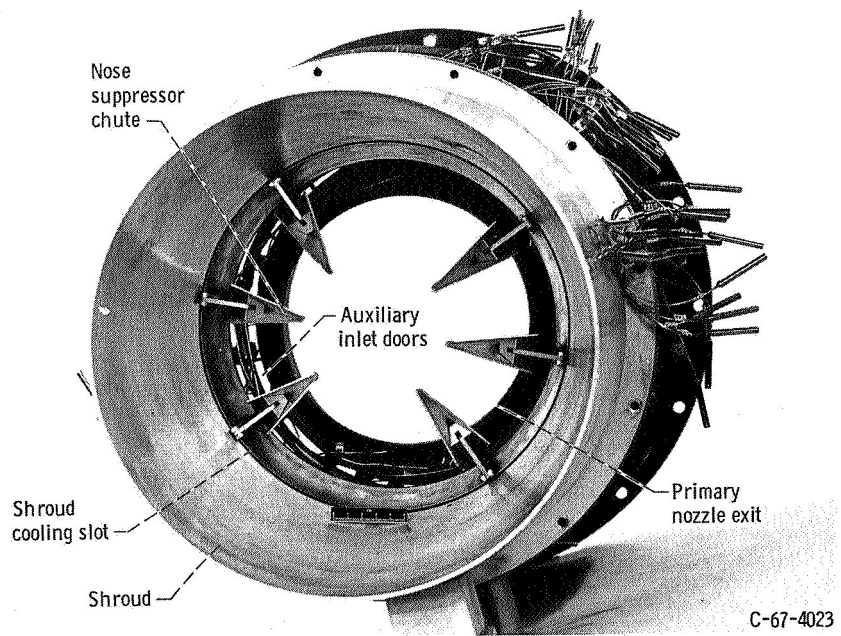
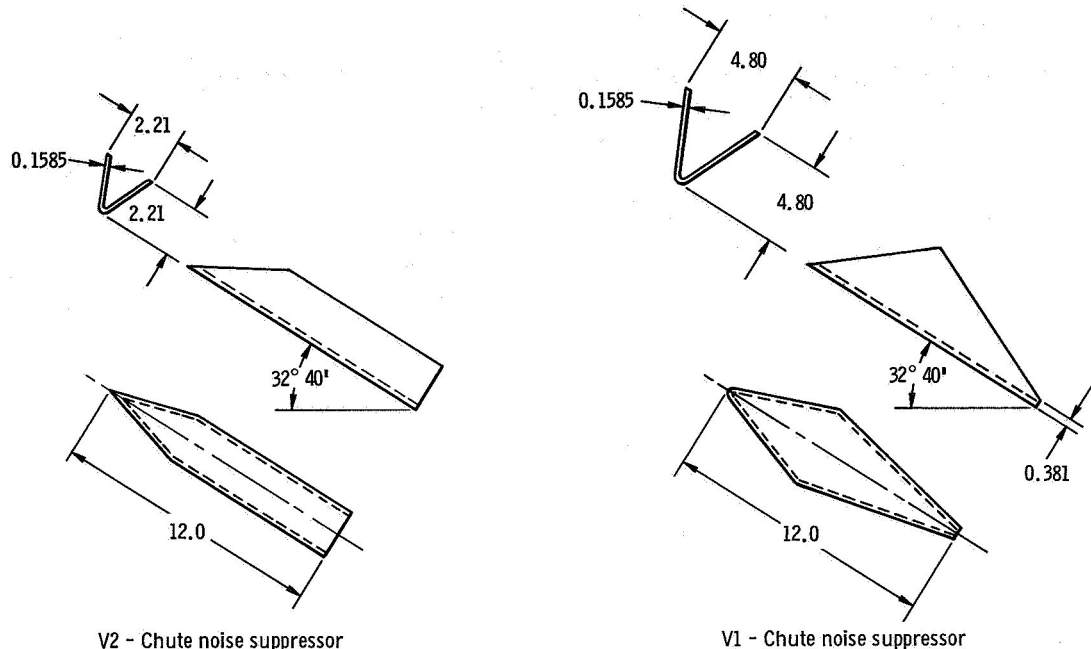
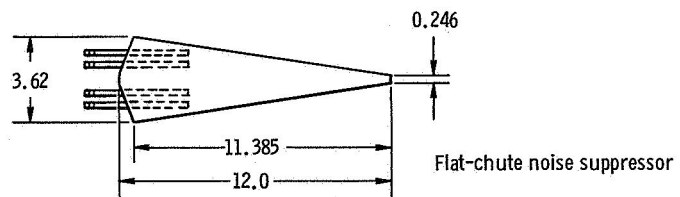


Figure 5. - Aft view of auxiliary inlet ejector nozzle assembly.



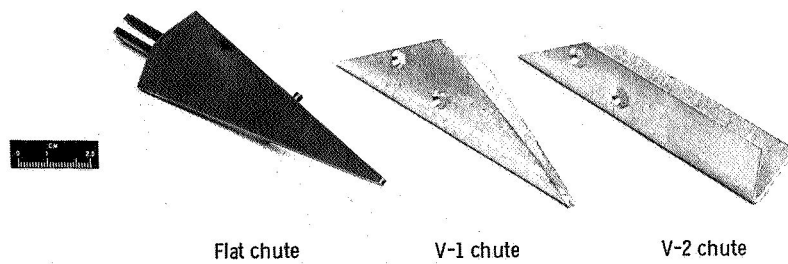
V2 - Chute noise suppressor

V1 - Chute noise suppressor



(a) Details of chute geometries.

CD -9865-28



Flat chute

V-1 chute

V-2 chute

C-67-4025

(b) Actual chute geometries.

Figure 6. - Noise suppressor chutes. (All dimensions in centimeters.)

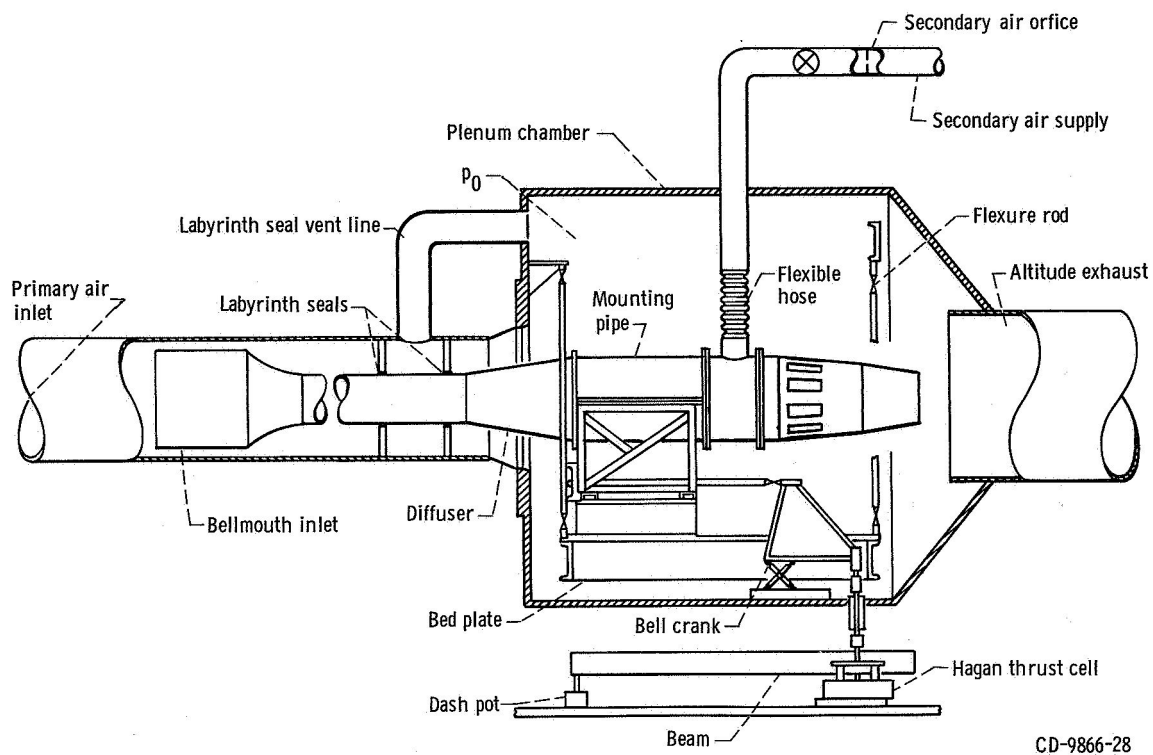


Figure 7. - Schematic of test stand showing nozzle support and air supply systems.

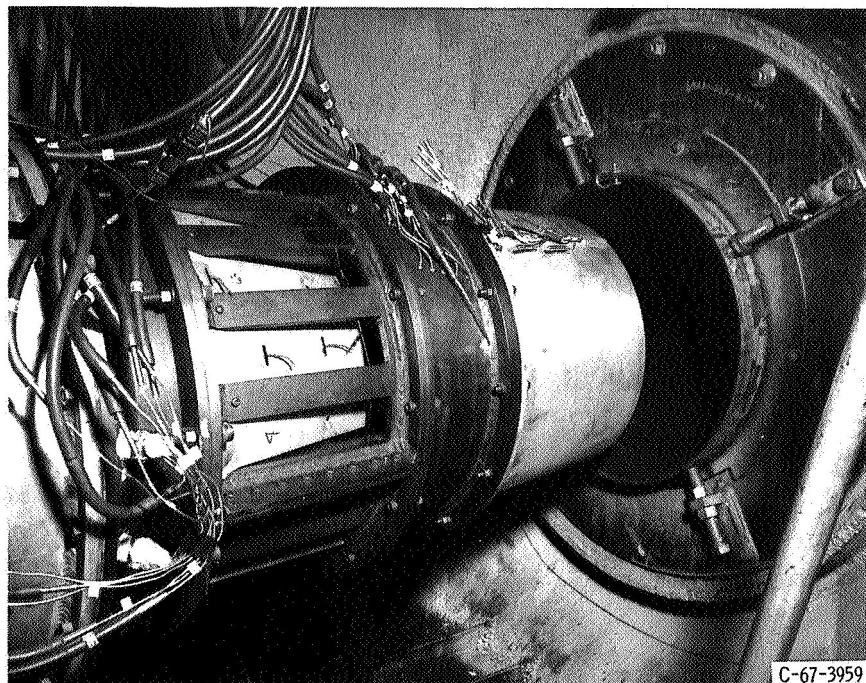
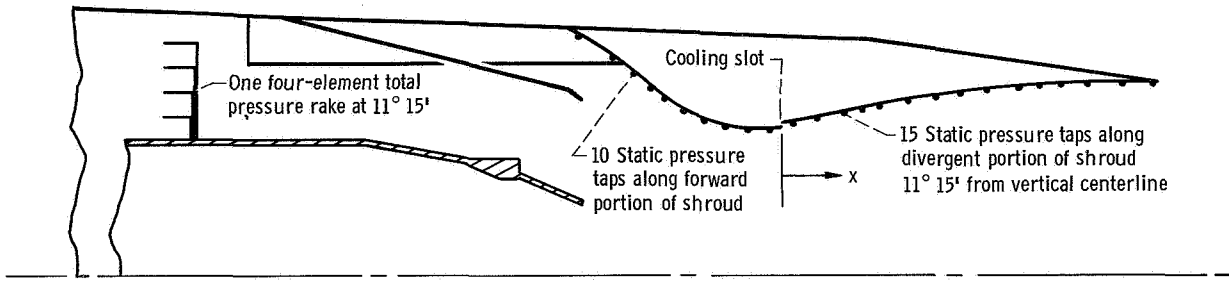


Figure 8. - Ejector nozzle installed in static test facility.



CD-9867-28

Forward shroud		Divergent shroud	
Tap	Axial distance	Tap	Axial distance
		$a_{x_1}$	$b_{x_2}$
1	-13.70	1	0.46
2	-12.69	2	1.78
3	-11.55	3	3.10
4	-10.45	4	4.47
5	-9.44	5	5.97
6	-8.04	6	7.47
7	-5.75	7	9.12
8	-4.36	8	10.60
9	-2.28	9	12.40
10	-.244	10	14.10
		11	15.87
		12	17.65
		13	19.42
		14	21.40
		15	23.10

<sup>a</sup>Used for shrouds 1, 5, and 6.  
<sup>b</sup>Used for shrouds 2, 3, and 4.  
<sup>c</sup>Forward from aft end.

Figure 9. - Auxiliary inlet ejector instrumentation layout. (All dimensions in centimeters.)

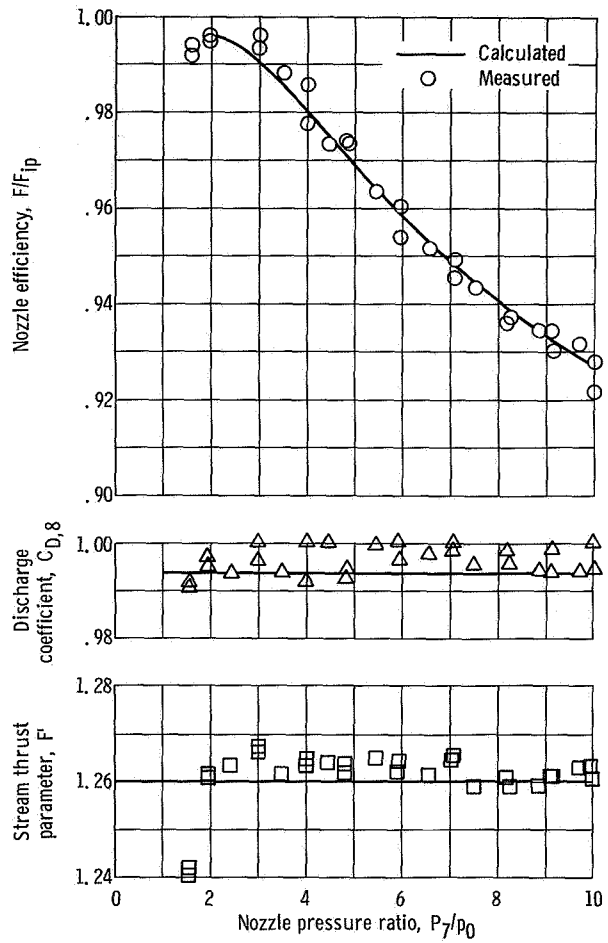
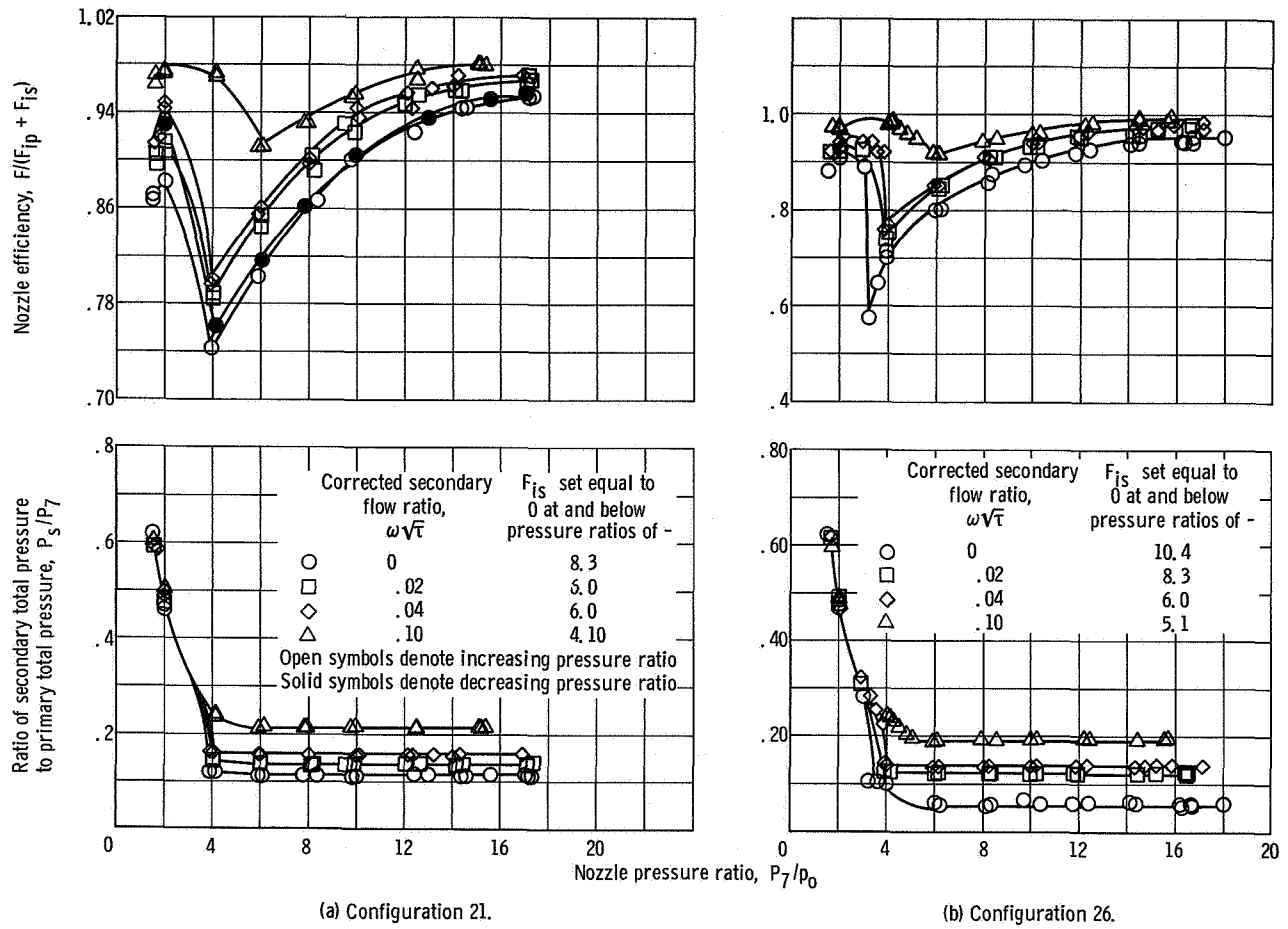


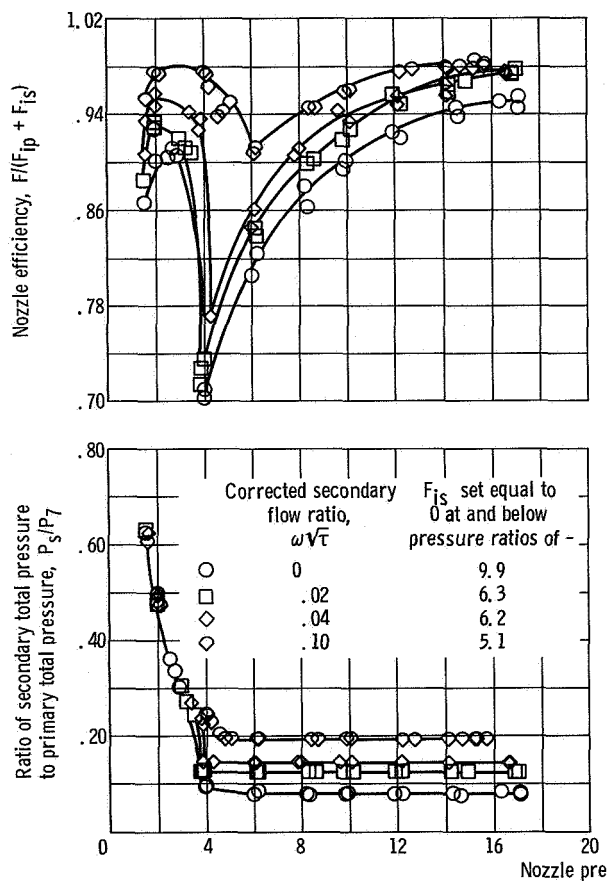
Figure 10. - Performance characteristics of 21.34-centimeter ASME nozzle.



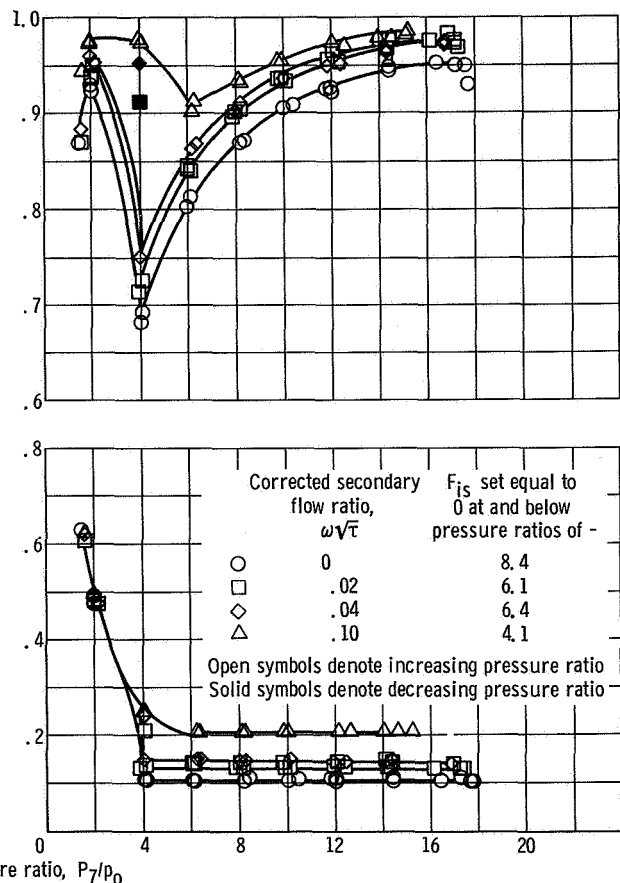
(a) Configuration 21.

(b) Configuration 26.

Figure 11. - Performance characteristics of auxiliary inlet ejector nozzle, supersonic cruise.

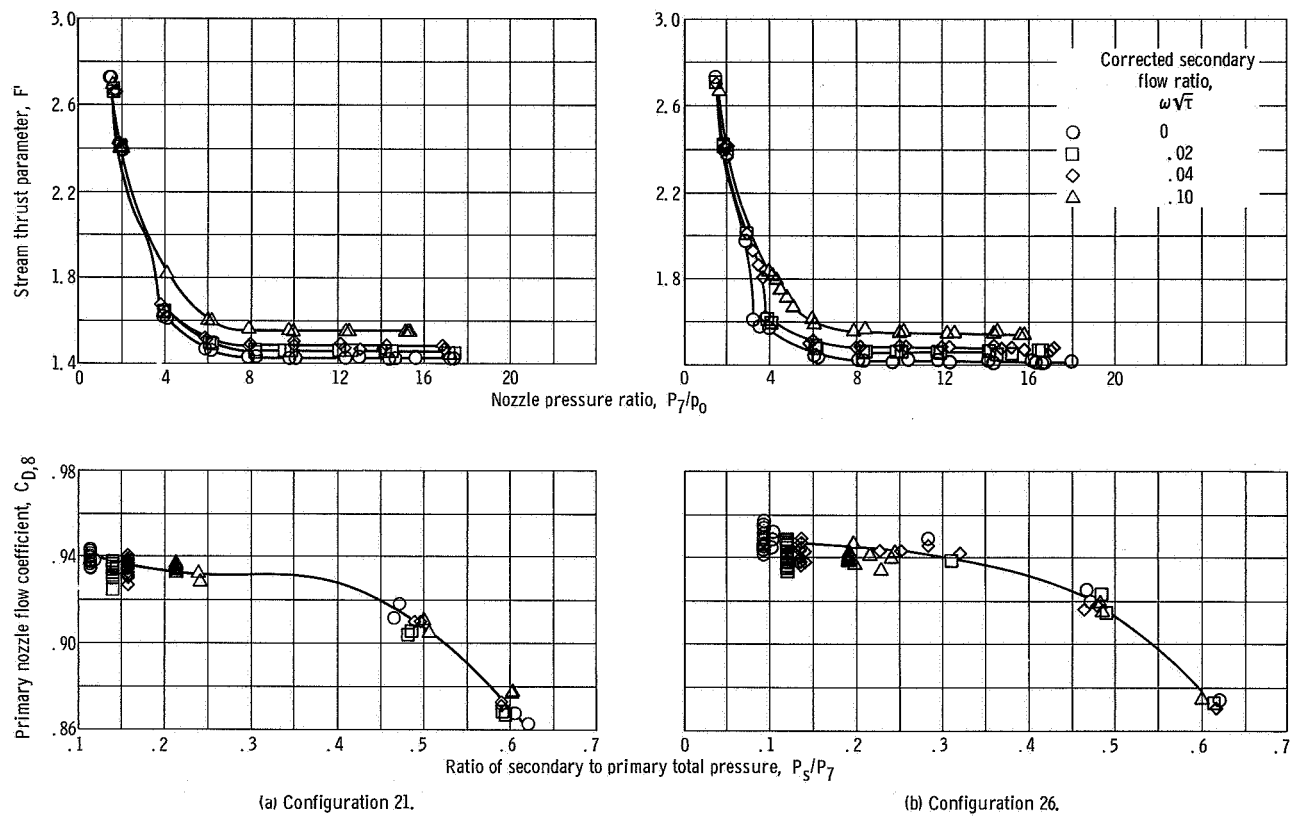


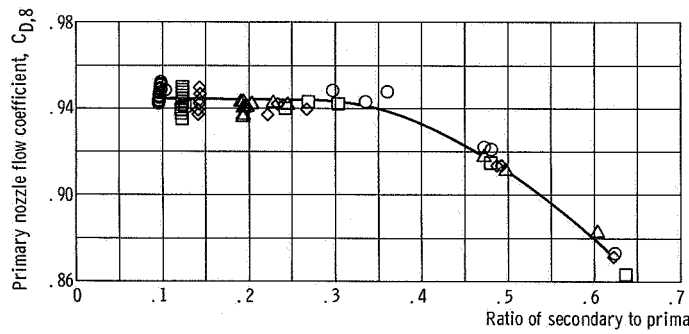
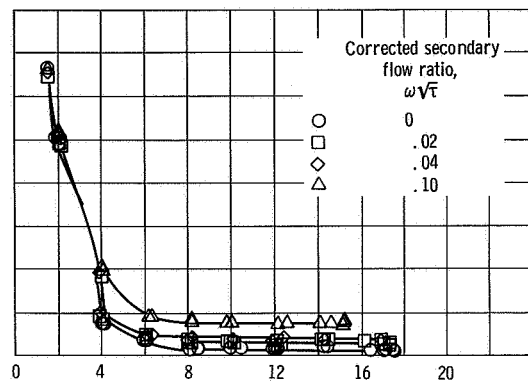
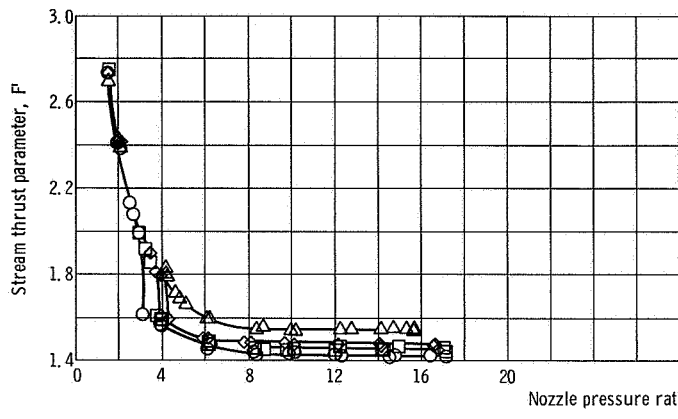
(c) Configuration 25.



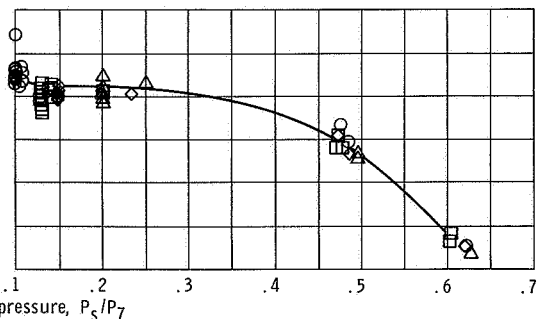
(d) Configuration 25, slot plugged.

Figure 11. - Concluded.





(c) Configuration 25.



(d) Configuration 25, cooling slot plugged.

Figure 12. - Concluded.

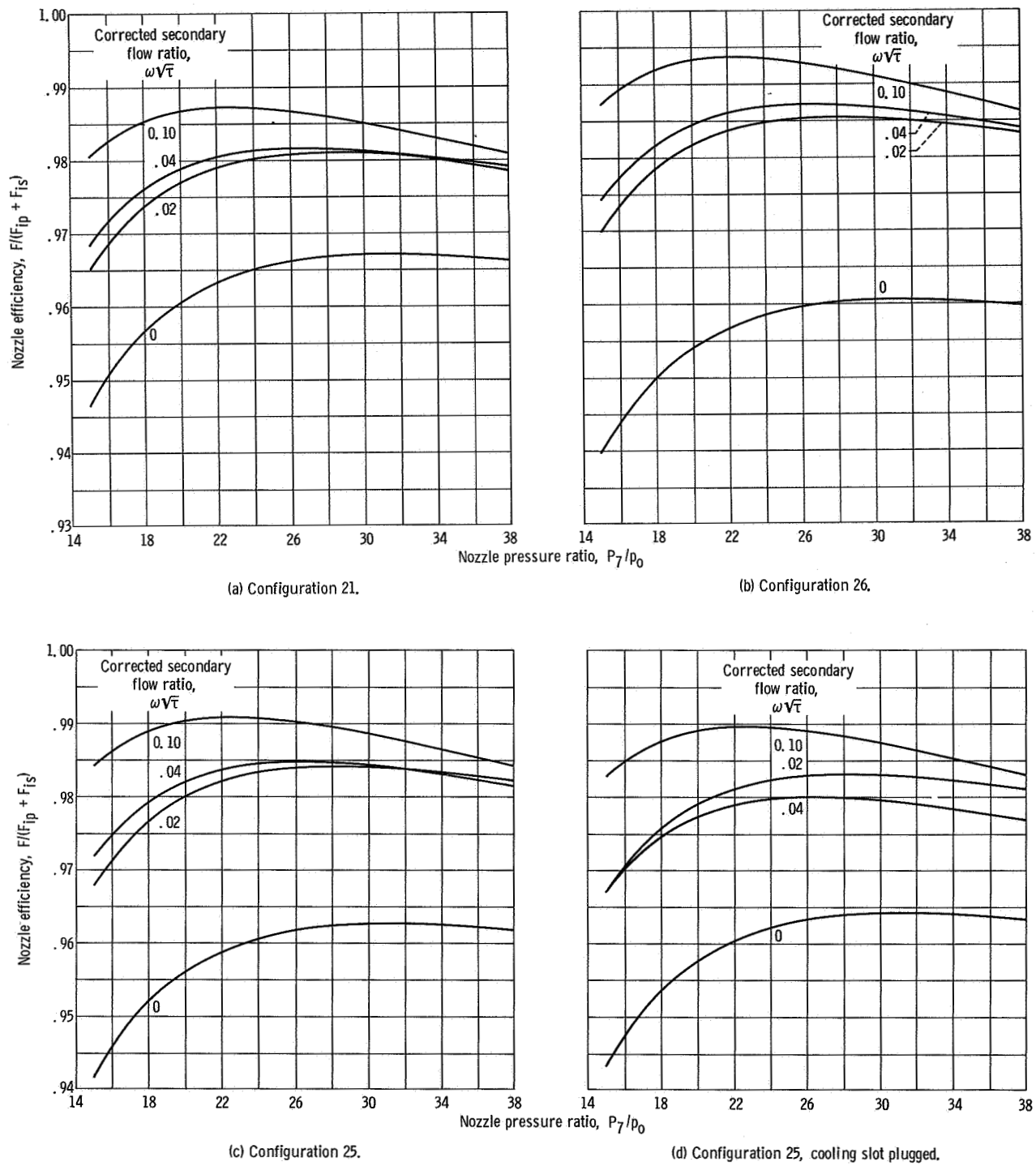


Figure 13. - Extrapolated performance of auxiliary inlet nozzle, supersonic cruise.

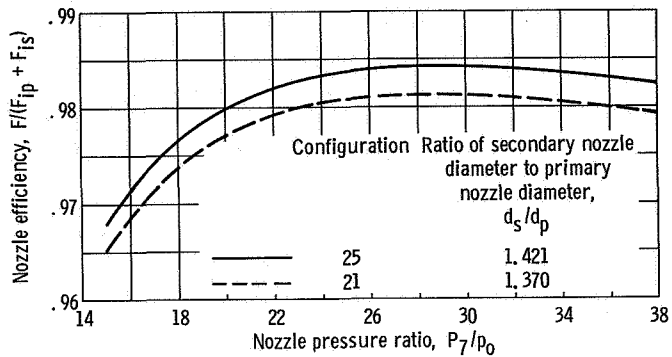


Figure 14. - Effect of internal shroud diameter on extrapolated performance. Corrected secondary flow ratio, 0.02; supersonic cruise configuration.

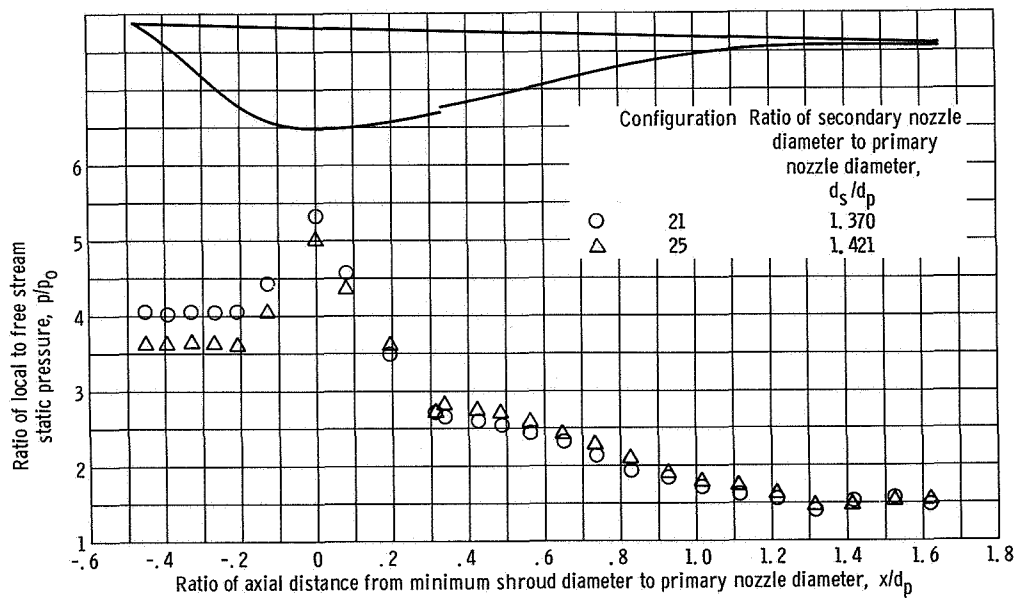


Figure 15. - Effect of internal shroud diameter on internal pressure distribution at design pressure ratio of 28.9. Corrected secondary flow ratio, 0.02.

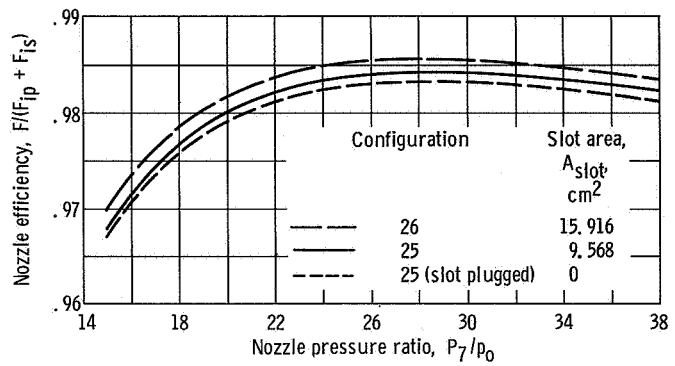


Figure 16. - Effect of cooling slot size on extrapolated performance.  
Corrected secondary flow ratio, 0.02.

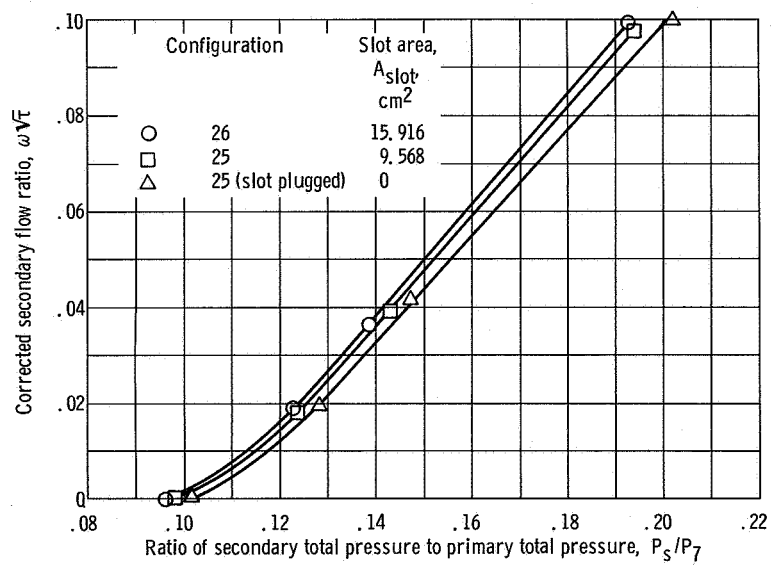
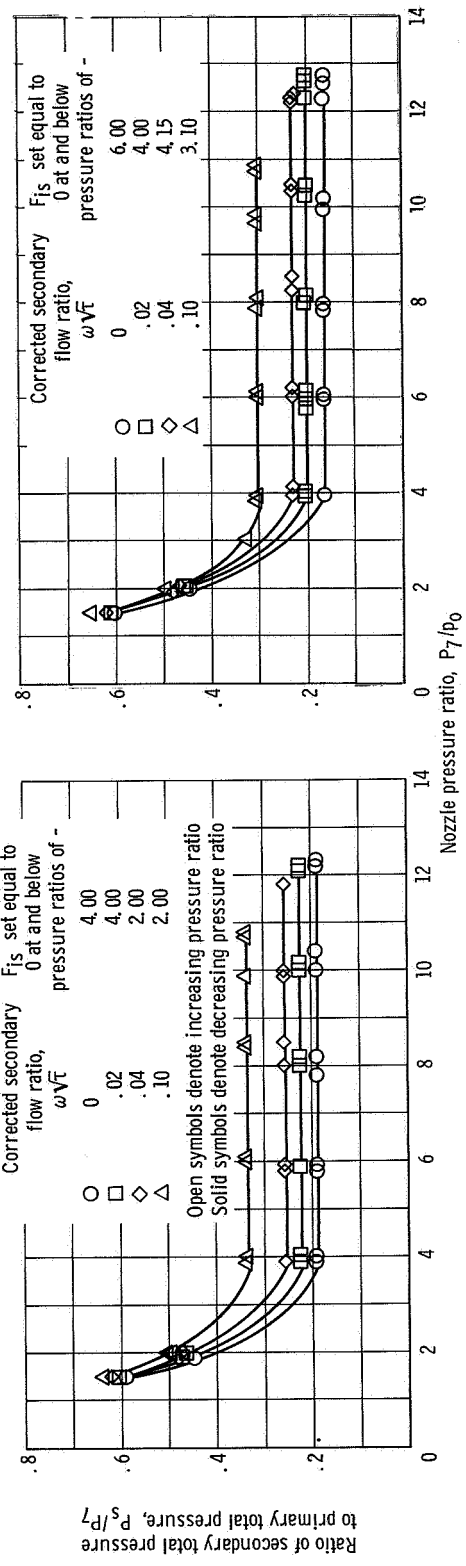
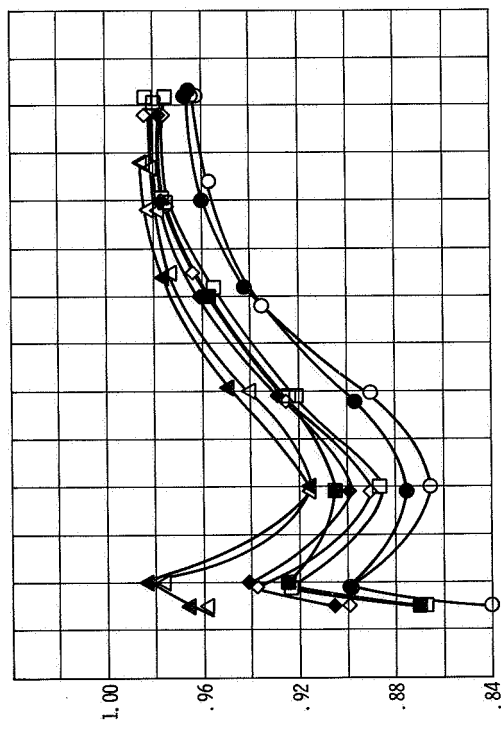
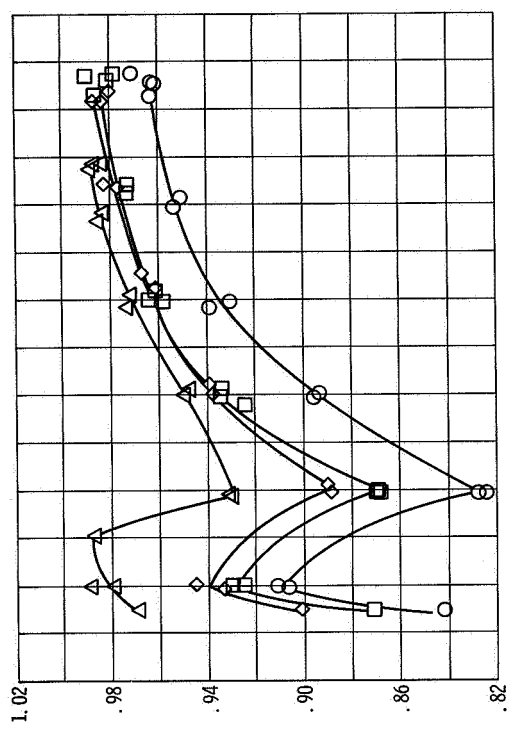


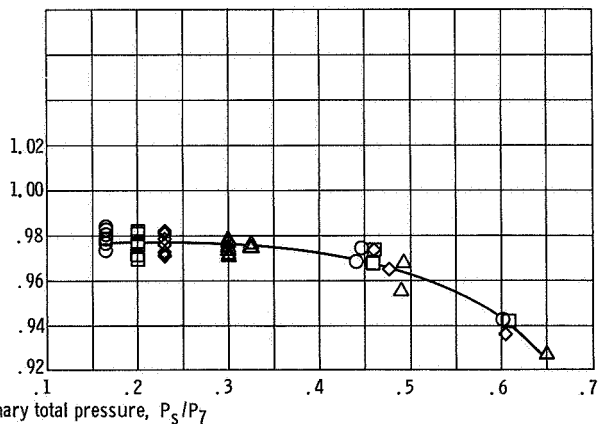
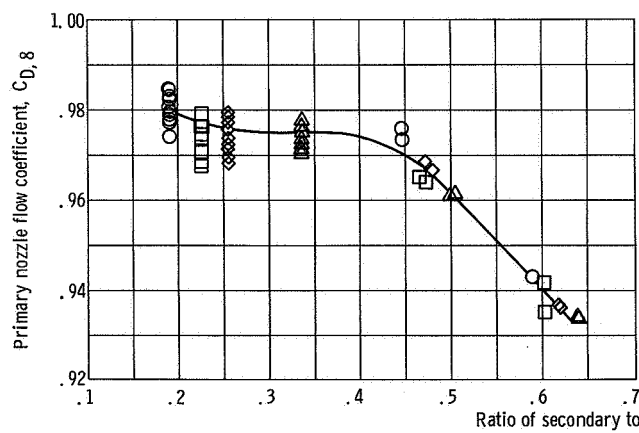
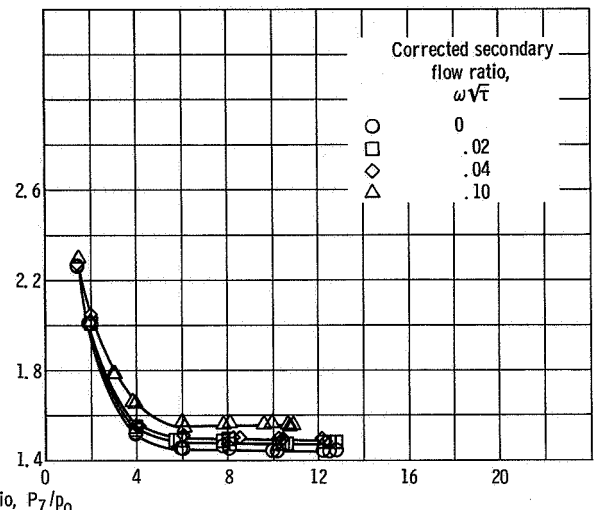
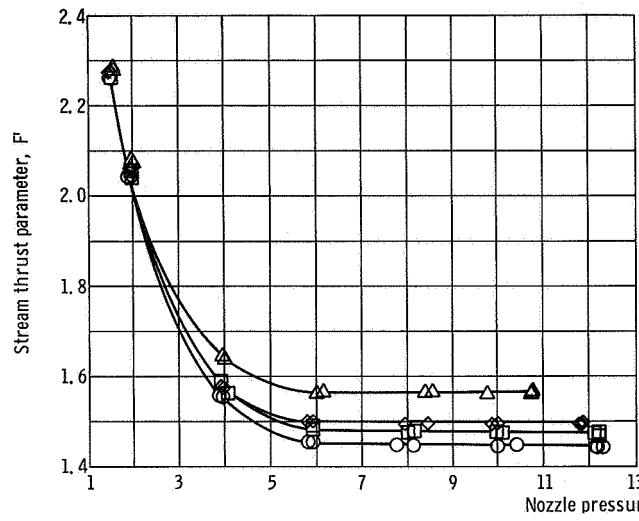
Figure 17. - Effect of cooling slot size on pumping characteristics of auxiliary inlet ejector nozzle at design pressure ratio.



(a) Configuration 11.

(b) Configuration 15.

Figure 18. - Performance characteristics of auxiliary inlet ejector nozzle, supersonic acceleration.



(a) Configuration 11.

(b) Configuration 15.

Figure 19. - Stream thrust parameters and nozzle flow coefficients for auxiliary inlet ejector nozzle.

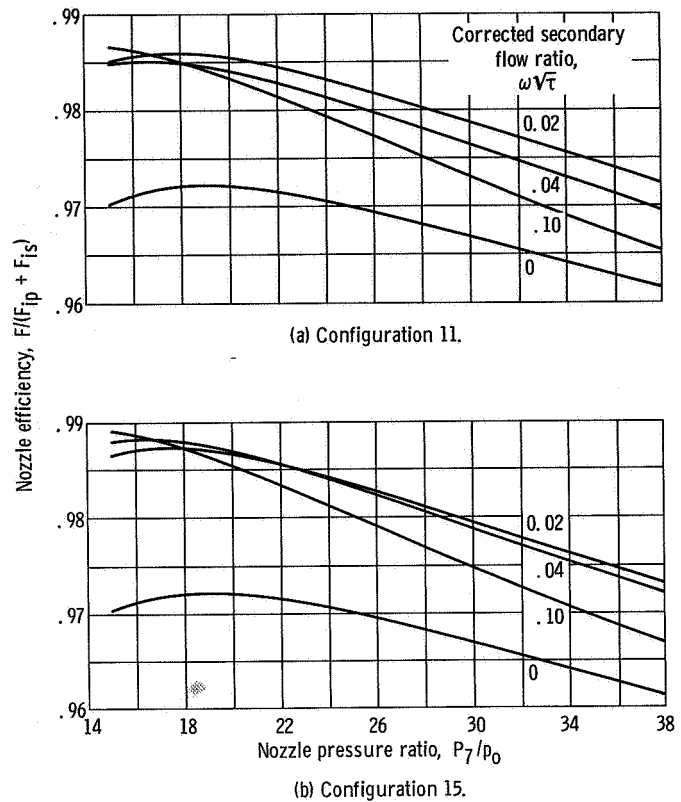


Figure 20. - Extrapolated performance of auxiliary inlet ejector nozzle.

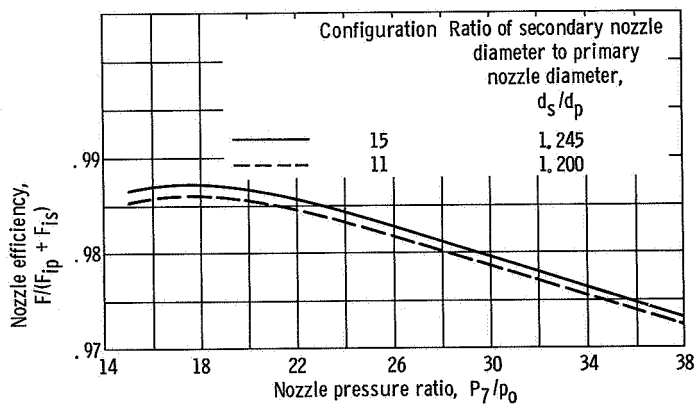
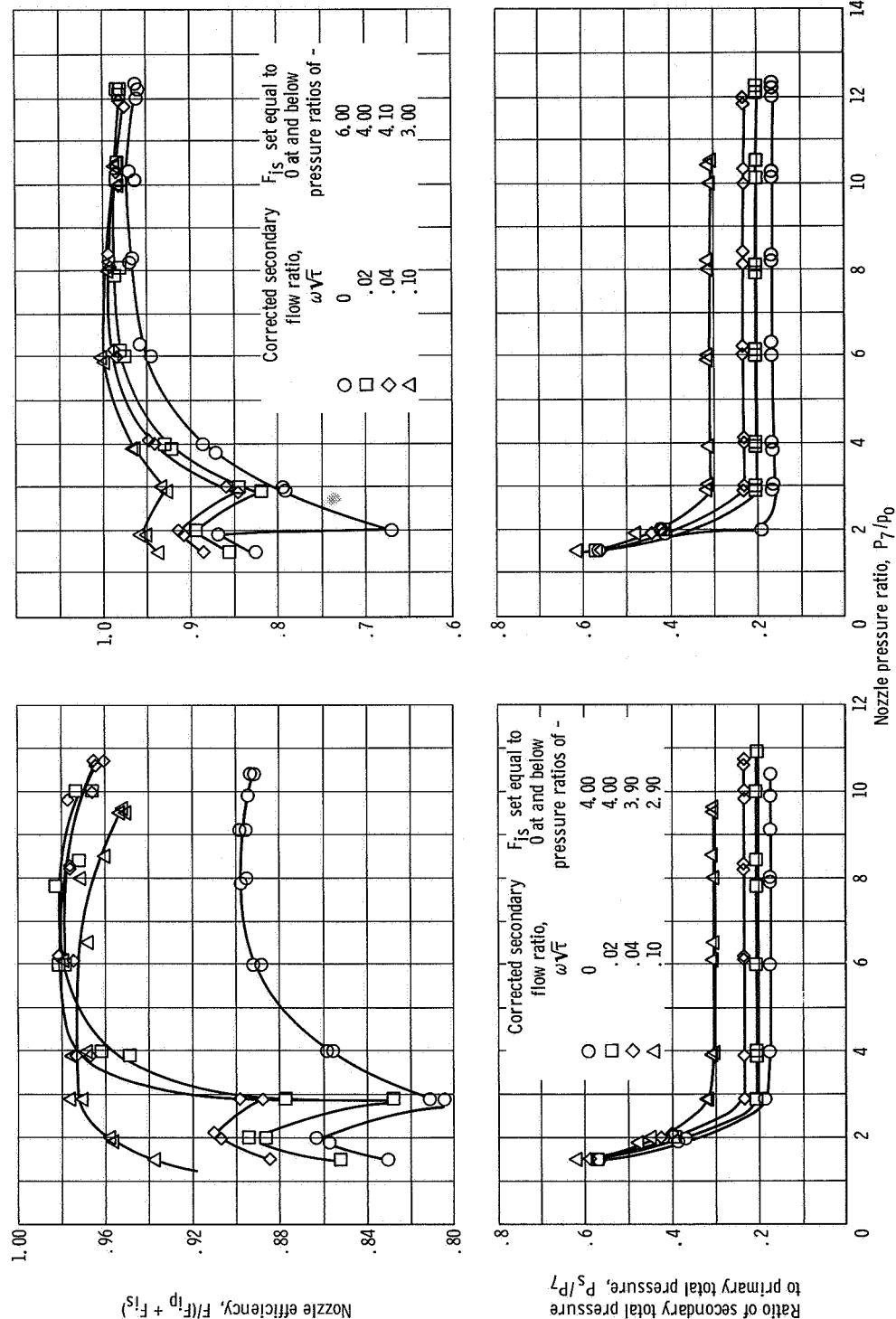


Figure 21. - Effect of internal shroud diameter on extrapolated performance. Corrected secondary flow ratio, 0.02; super-sonic acceleration configuration.



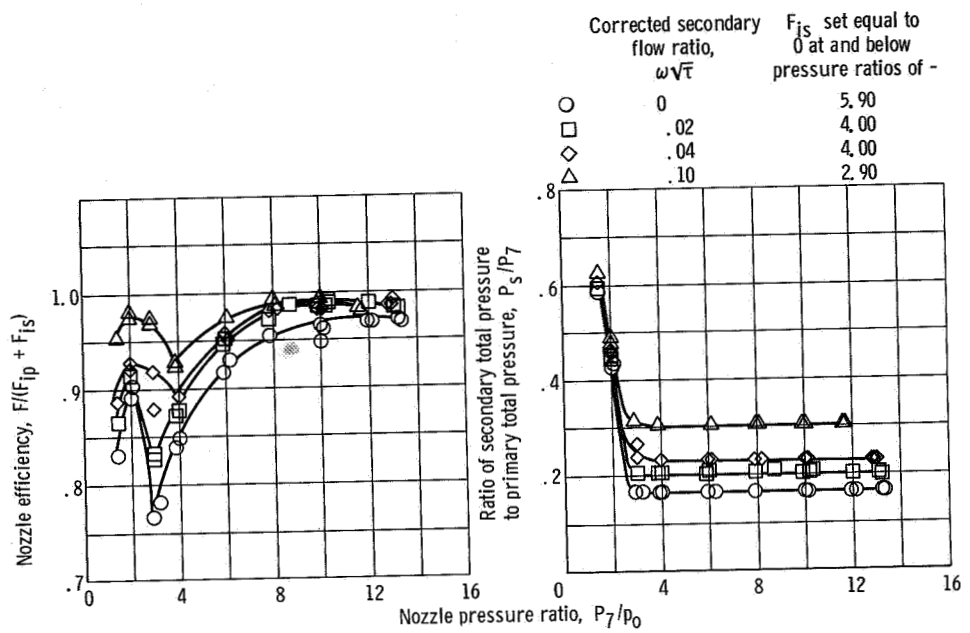
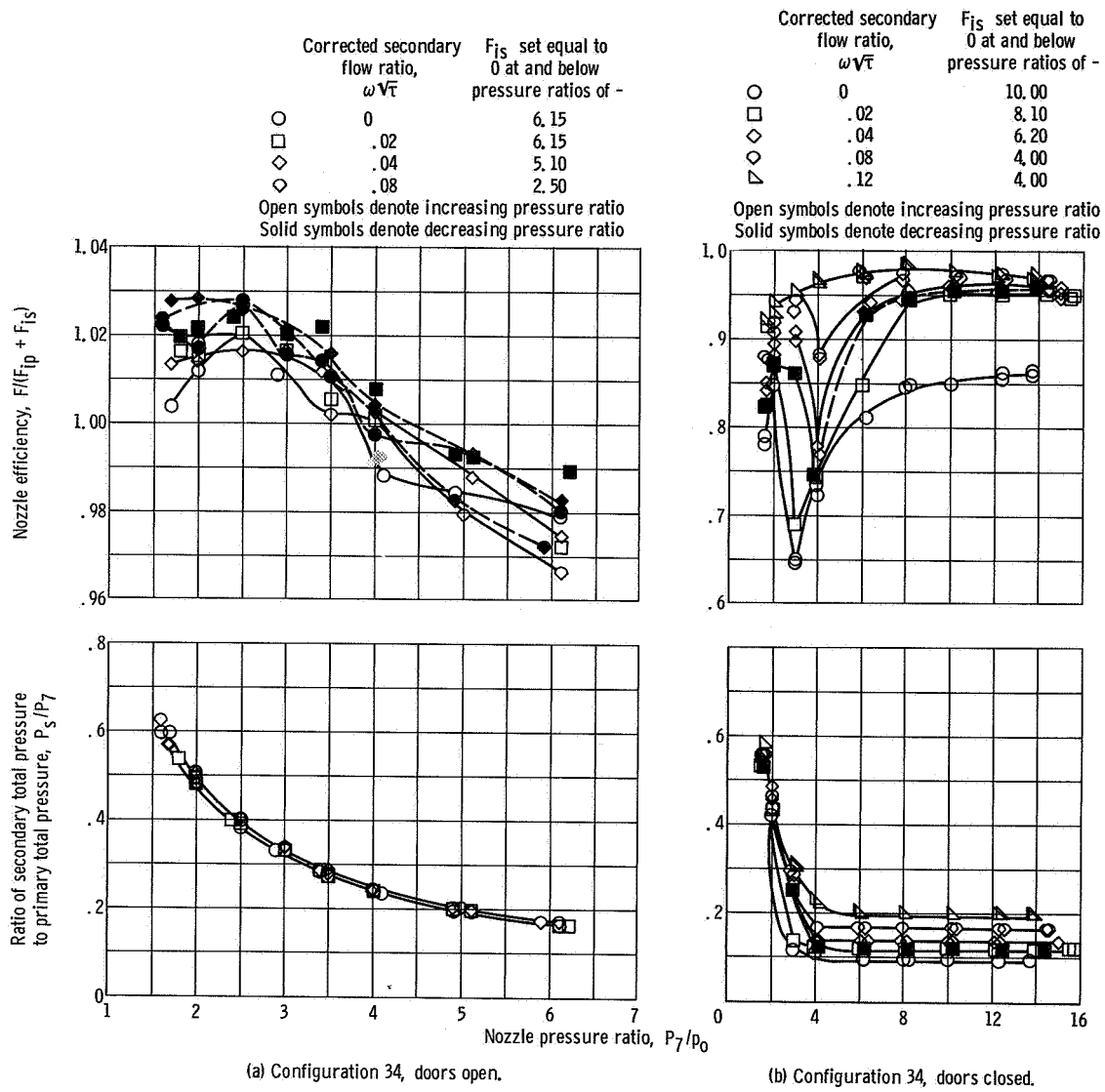


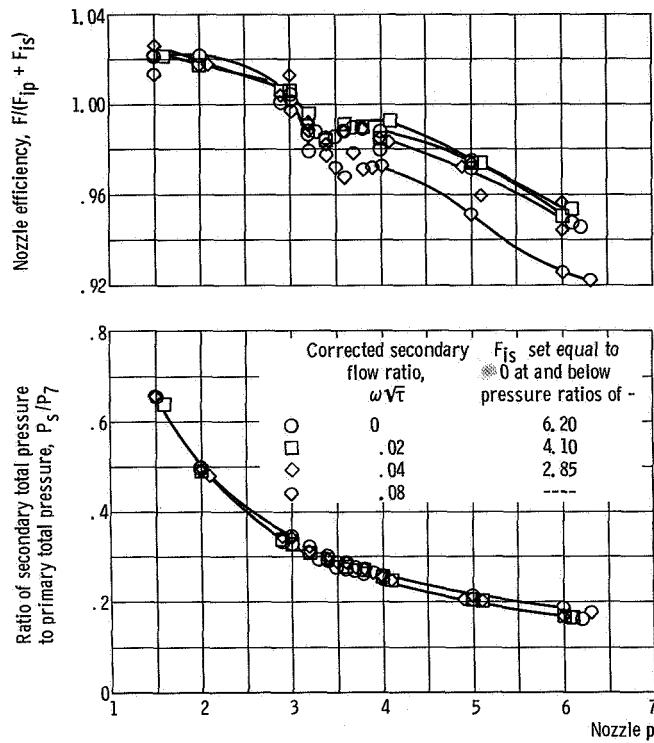
Figure 22. - Concluded.



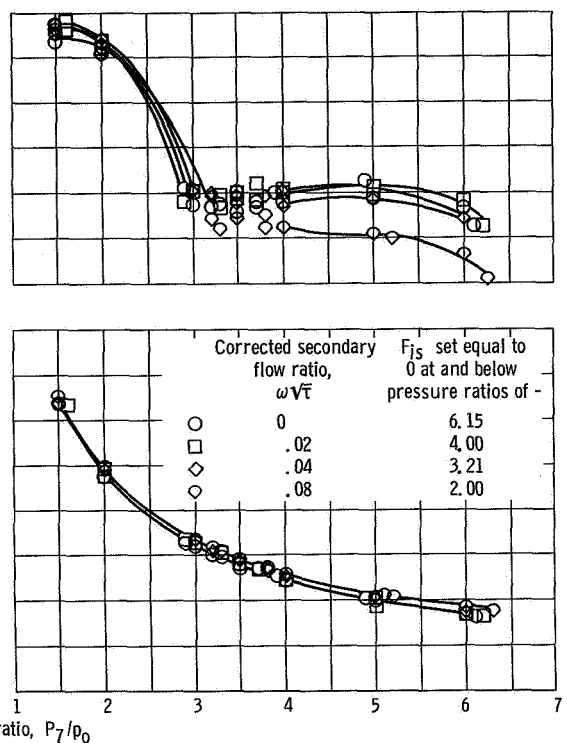
(a) Configuration 34, doors open.

(b) Configuration 34, doors closed.

Figure 23. - Performance characteristics of auxiliary inlet ejector nozzle, takeoff configurations.

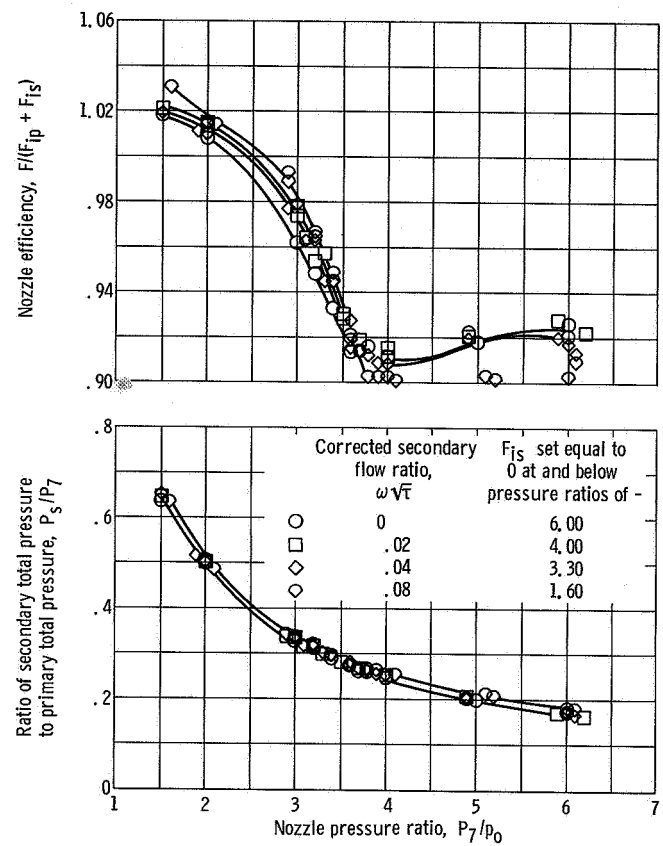


(c) Configuration 14, doors open.



(d) Configuration 13, doors open.

Figure 23. - Continued.



(e) Configuration 12, doors open.

Figure 23. - Concluded.

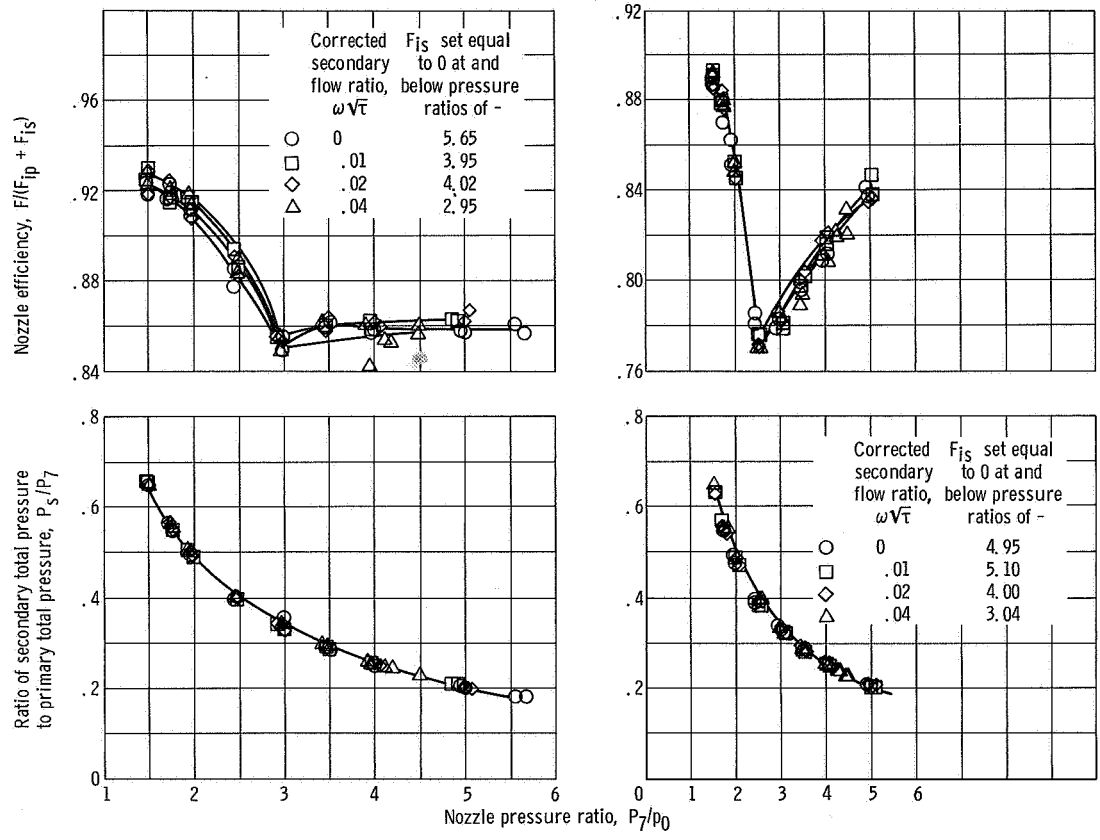
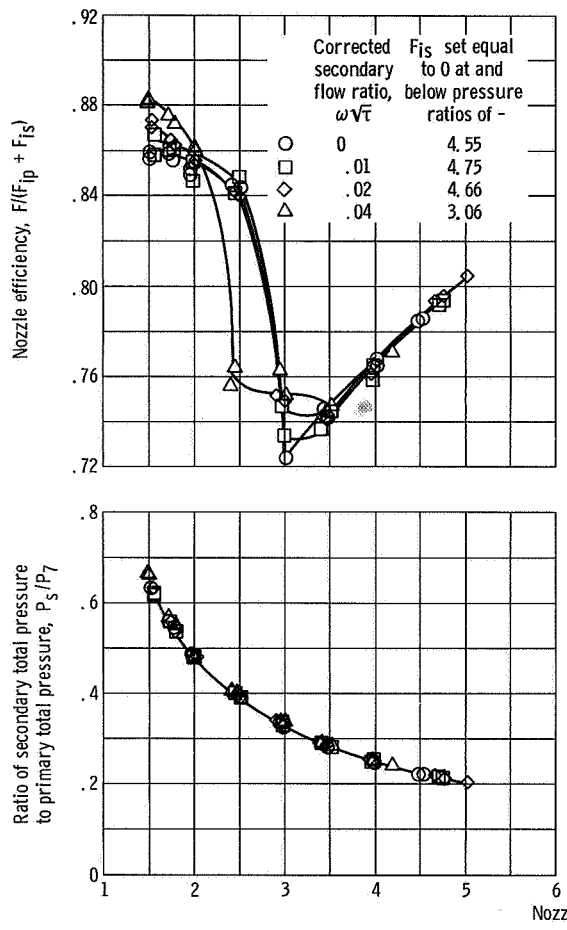
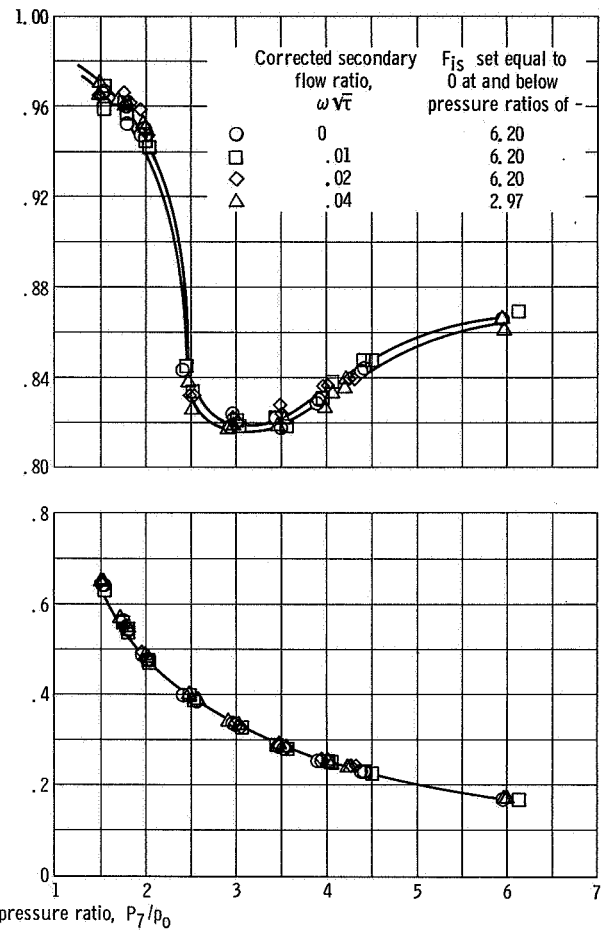


Figure 24. - Performance characteristics of auxiliary inlet ejector nozzle, takeoff with noise suppression.

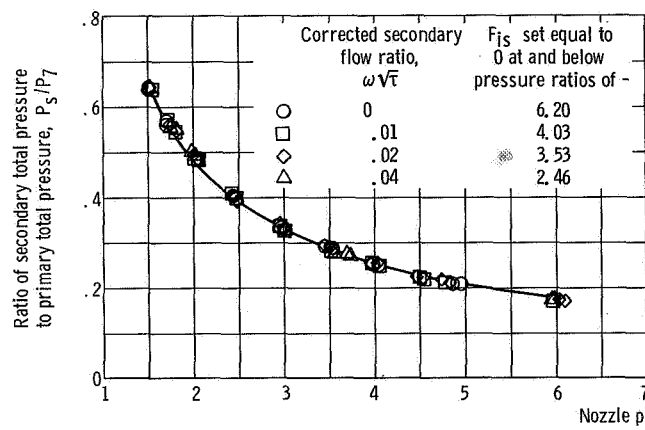
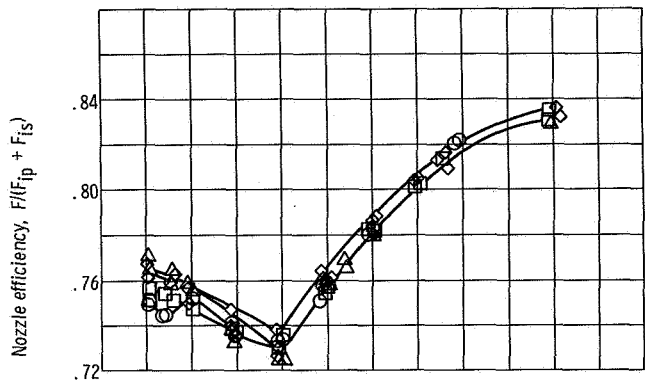


(c) Configuration 15. Flat noise suppressor chute; chute angle,  $32^{\circ}40'$ .

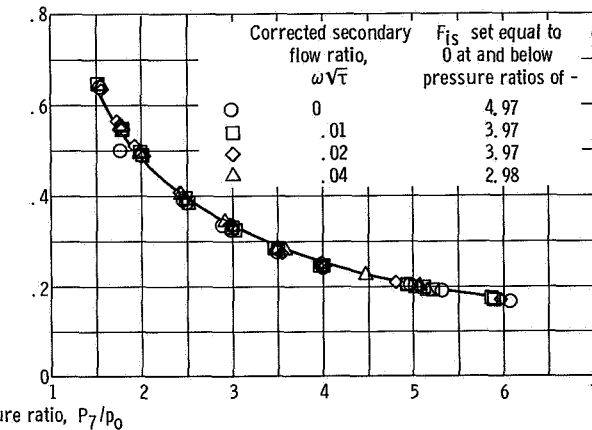
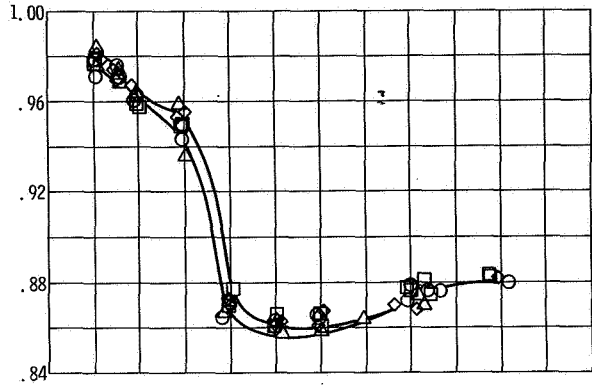


(d) Configuration 12. Noise suppressor chute angle,  $25^{\circ}$ .

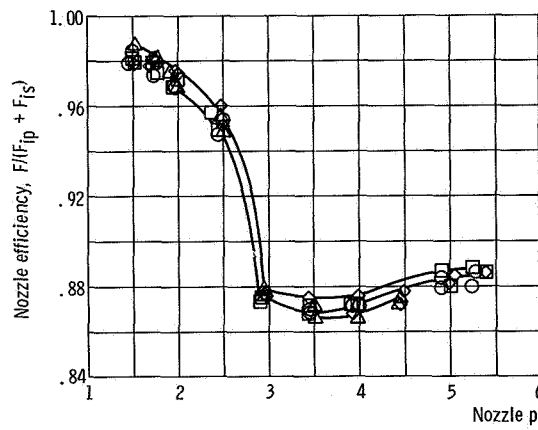
Figure 24. - Continued.



(e) Configuration 12. Flat noise suppressor chute; chute angle,  $40^\circ$ .



(f) Configuration 12. V1 noise suppressor chute; chute angle,  $32^\circ 40'$ .



(g) Configuration 12. V2 noise suppressor chute; chute angle,  $32^\circ 40'$ .

Figure 24. - Concluded.

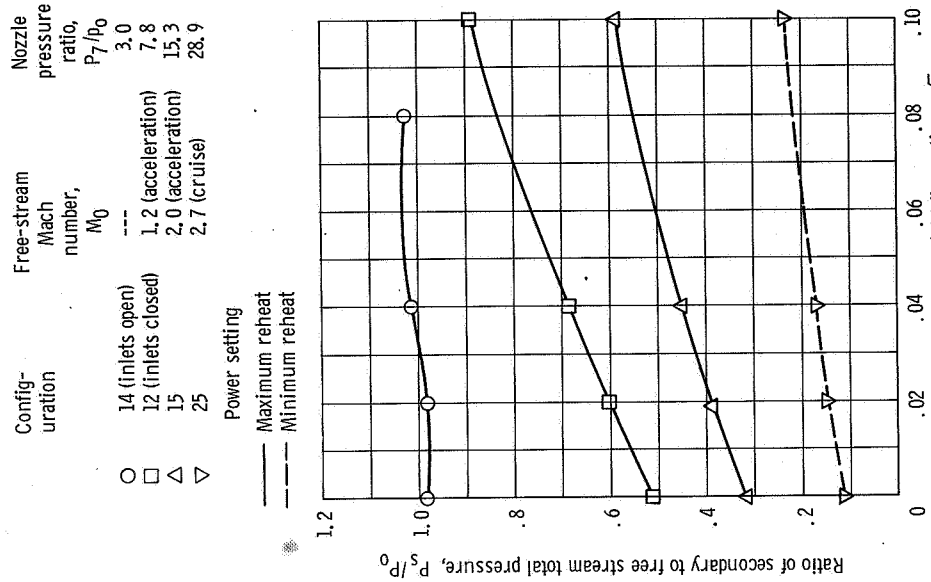


Figure 26. - Secondary total pressure recovery requirements for auxiliary inlet ejector.

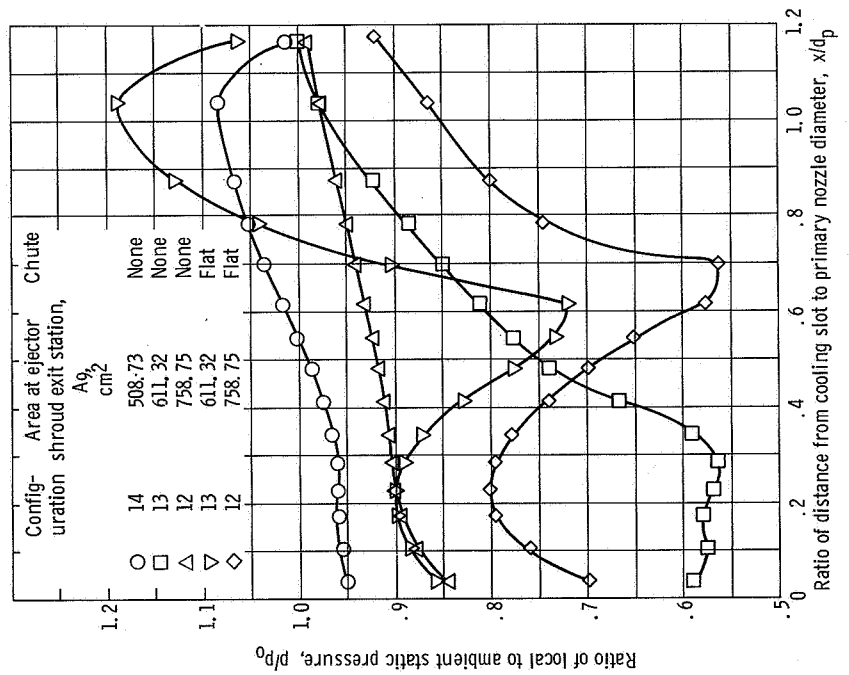


Figure 25. - Effect of noise suppressor chutes on secondary shroud pressure distribution. Nozzle pressure ratio, 3.0; secondary flow, 0.04; flat noise suppressor chute; chute angle, 32°40'.

NATIONAL AERONAUTICS AND SPACE ADMINISTRATION  
WASHINGTON, D.C. 20546

OFFICIAL BUSINESS

POSTAGE AND FEES PAID  
NATIONAL AERONAUTICS AND  
SPACE ADMINISTRATION

FIRST CLASS MAIL

POSTMASTER If Undeliverable (Section 156  
Postal Manual) Do Not Return

*"The aeronautical and space activities of the United States shall be conducted so as to contribute . . . to the expansion of human knowledge of phenomena in the atmosphere and space. The Administration shall provide for the widest practicable and appropriate dissemination of information concerning its activities and the results thereof."*

— NATIONAL AERONAUTICS AND SPACE ACT OF 1958

## NASA SCIENTIFIC AND TECHNICAL PUBLICATIONS

**TECHNICAL REPORTS:** Scientific and technical information considered important, complete, and a lasting contribution to existing knowledge.

**TECHNICAL NOTES:** Information less broad in scope but nevertheless of importance as a contribution to existing knowledge.

**TECHNICAL MEMORANDUMS:** Information receiving limited distribution because of preliminary data, security classification, or other reasons.

**CONTRACTOR REPORTS:** Scientific and technical information generated under a NASA contract or grant and considered an important contribution to existing knowledge.

**TECHNICAL TRANSLATIONS:** Information published in a foreign language considered to merit NASA distribution in English.

**SPECIAL PUBLICATIONS:** Information derived from or of value to NASA activities. Publications include conference proceedings, monographs, data compilations, handbooks, sourcebooks, and special bibliographies.

**TECHNOLOGY UTILIZATION PUBLICATIONS:** Information on technology used by NASA that may be of particular interest in commercial and other non-aerospace applications. Publications include Tech Briefs, Technology Utilization Reports and Notes, and Technology Surveys.

*Details on the availability of these publications may be obtained from:*

**SCIENTIFIC AND TECHNICAL INFORMATION DIVISION  
NATIONAL AERONAUTICS AND SPACE ADMINISTRATION**

Washington, D.C. 20546